Title: Cluster II *che* genes of *Pseudomonas syringae* pv. *tabaci* 6605, orthologs of cluster I in *Pseudomonas aeruginosa,* are required for chemotaxis and virulence

Authors' names: Stephany Angelia Tumewu[1], Yujiro Ogawa[2], Takumi Okamoto[2], Yuka Sugihara[2], Hajime Yamada[2], Fumiko Taguchi[1,3], Hidenori Matsui[1], Mikihiro Yamamoto[1], Yoshiteru Noutoshi[1], Kazuhiro Toyoda[1] and Yuki Ichinose[1,]*.

Affiliation and address:

[1] Graduate School of Environmental and Life Science, Okayama University, Tsushima-naka 1-1-1, Kita-ku, Okayama 700-8530, Japan

[2] Faculty of Agriculture, Okayama University, Tsushima-naka 1-1-1, Kita-ku, Okayama 700-8530, Japan

[3] Present Address: Department of Biotechnology, Graduate School of Engineering, Nagoya University, Furo-cho, Chikusa-ku, Nagoya 464-8603, Japan

***For correspondence:** E-mail, yuki@okayama-u.ac.jp; Tel/Fax: (+81) 86 251 8308.

Number of figures and tables: 6 figures, 2 tables (6 supplemental figures)

Word count: 8869

Abstract (196 words)

Pseudomonas syringae pv. *tabaci* 6605 (*Pta*6605) is a causal agent of wildfire disease in host tobacco plants and is highly motile. *Pta*6605 has multiple clusters of chemotaxis genes including *cheA*, a gene encoding a histidine kinase, *cheY*, a gene encoding a response regulator, *mcp,* a gene for a methyl-accepting chemotaxis protein, as well as flagellar and pili biogenesis genes. However, only two major chemotaxis gene clusters, cluster I and cluster II, possess *cheA* and *cheY*. Deletion mutants of *cheA* or *cheY* were constructed to evaluate their possible role in *Pta*6605 chemotaxis and virulence. Motility tests and a chemotaxis assay to known attractant demonstrated that *cheA2* and *cheY2* mutants were unable to swarm and to perform chemotaxis, whereas *cheA1* and *cheY1* mutants retained chemotaxis ability almost equal to that of the wild-type (WT) strain. Although WT and *cheY1* mutants of *Pta*6605 caused severe disease symptoms on host tobacco leaves, the *cheA2* and *cheY2* mutants did not, and symptom development with *cheA1* depended on the inoculation method. These results indicate that chemotaxis genes located in cluster II are required for optimal chemotaxis and host plant infection by *Pta*6605 and that cluster I may partially contribute to these phenotypes.

Keywords: bacterial virulence, *cheA*, chemotaxis, *cheY*, flagellar motility, *Pseudomonas*

Introduction

Pseudomonas syringae is a model of foliar plant bacterial pathogens, which comprises about 50 pathovars based on its diverse interaction with their host plants, epiphytic survival, and the nature of the elicited disease symptoms (Xin et al. 2018). *P. syringae* pv. *tabaci* 6605 (*Pta*6605) is one of the *P. syringae* strains that causes wildfire disease on tobacco plants (Ichinose et al. 2003). To infect host plants, *P. syringae* requires several virulence factors including an Hrp type III secretion system, phytotoxins, quorum-sensing, and flagella- and type IV pili-mediated motilities (Ichinose et al. 2003, 2013; Kanda et al. 2011; Taguchi and Ichinose, 2011).

Pathogen entry into plant apoplastic spaces is a first key point for successful invasion and escaping the harsh environment on the leaf surface (Melotto et al. 2006). Unlike fungal pathogens that can directly penetrate the epidermis, foliar bacterial pathogens like *P. syringae* need to enter through natural openings such as stomata, wounds, or hydathodes. The ability of *P. syringae* pv. *tomato* DC3000 (*Pto*DC3000), *Salmonella enterica*, and *Dickeya dadantii* to preferably move toward open stomata and wounding sites has been reported (Antunnez-Lamas et al. 2009; Kroupitski et al. 2009; Melotto et al. 2006). Nevertheless, how bacteria navigate on the leaf surface and locate natural opening sites is still poorly understood.

Chemotaxis is a way for plant-pathogenic bacteria to sense and respond to chemicals released from plant tissues to the leaf surface, and hence ensures survival and pathogenicity (Yao and Allen 2006). Chemotaxis itself is the movement of an organism toward or away from a chemical stimulus. Motile bacteria can sense changes in the concentration of chemicals in their environments and respond to the changes by altering their motility pattern (Sourjik and Wingreen 2012). Genetic analysis of the chemotaxis behavior has been studied extensively in

Escherichia coli, *S. enterica*, and *Pseudomonas aeruginosa* (Blair 1995; Bi and Lai 2015; Kato et al. 1999; Manson 1992).

Comparative genomics of *Pto*DC3000 revealed that this foliar plant pathogen possesses at least two major chemotaxis-related gene clusters (Buell et al. 2003; Clarke et al. 2016). There are genes encoding two histidine kinases, CheA1 and CheA2, and two response regulators, CheY1 and CheY2. CheA and CheY are essential for a two-component phosphorelay system, enabling the bacteria cells to perform taxis toward chemical stimuli. Binding of a chemotactic signal to a chemoreceptor produces downstream information that modulates the histidine kinase CheA autophosphorylation activity. CheA will be autophosphorylated at specific histidine residues to form CheA-P. A phosphoryl group from CheA-P will be transferred to a specific aspartate residue of CheY to form active CheY-P, which is a response regulator of a two-component regulatory system. CheY-P interacts directly with a flagellar motor switch protein to control the direction of the flagellar rotation, namely clockwise or counter-clockwise (Wadhams and Armitage 2004).

*Pta*6605 shows high motility and virulence (Taguchi et al. 2010; Taguchi and Ichinose 2011), making it a suitable model for studying the role of chemotaxis in this species. The bacterial flagellum motor is a molecular machine that generates energy and rotates flagella. The motor complexes are composed of two stator proteins MotA and MotB or MotC and MotD. Genes *motA* and *motB* are tandemly located within a potential operon, whereas *motC* and *motD* are also tandemly located but in a different position from *motAB* on the chromosome. Previous study using Δ*motAB* and Δ*motCD* mutant strains demonstrated that MotCD is required for flagellar motility but not another stator protein MotAB (Kanda et al. 2011). Genes *motCD*,

cheA2, and *cheY2* are located in the same chemotaxis gene cluster (*che2*), whereas *cheA1* and *cheY1* are located in another chemotaxis gene cluster (*che1*, Fig. 1). Thus, in this study, to investigate how CheA and CheY contribute to *Pta*6605 motility and how chemotaxis affects the virulence of this strain, we generated the *Pta*6605 mutants *cheA1*, *cheA2*, *cheY1*, and *cheY2* from two chemotaxis gene clusters. Based on tests of chemotaxis toward a known attractant, *cheA2* and *cheY2* mutants lack chemotactic ability. Furthermore, the *cheA2* and *cheY2* mutants had reduced or altered surface motility. More importantly, they also had remarkably reduced virulence on host tobacco plants, which suggests that chemotaxis is indeed required for effective host plant colonization and that the chemotaxis required for virulence in *Pta*6605 is *che2* pathway–dependent. The nomenclature for chemotaxis genes is confusing: chemotaxis gene cluster I in *P. syringae* is an ortholog of chemotaxis gene cluster II in *P. aeruginosa*, whereas chemotaxis gene cluster II in *P. syringae* is an ortholog of chemotaxis gene cluster I in *P. aeruginosa* (Fig. 1, Clarke et al. 2016; Ferrández et al. 2002). To avoid confusion, we designated the former genes as a group II chemotaxis gene cluster and the latter genes as a group III chemotaxis gene cluster, as described below in the Results section.

Materials and methods

CheA and CheY phylogenetic analysis

We obtained the CheA and CheY amino acid sequences from previous reports that characterized chemotaxis genes functions from the Pseudomonas Genome Database and GeneBank. Bacteria strains included in the phylogenetic tree were *P. syringae* pv. *tabaci* 6605 (*Pta*6605), *P. syingae* pv. *phaseolicola* 1448a (*Pph*1448A) (Joardar et al. 2005), *P. syringae*

pv. *tomato* (*Pto*DC3000) (Buell et al. 2003), *P. fluorescens* F113 (Redondo-Nieto et al. 2011), *Ralstonia solanacearum* GMI1000 (Salanoubat et al. 2002), *P. aeruginosa* PAO1 (Stover *et al*. 2000), *Vibrio cholera* O395 (Feng et al. 2008), *S. enterica* serovar Typhimurium LT2 (McClelland et al. 2001), and *E. coli* K12 (Blattner et al. 1997). Amino acid sequences of CheA and CheY were aligned with ClustalW, and neighbor-joining trees were constructed based on the alignment using MEGA7 software.

Bacterial strains and growth condition

The bacterial strains used in this study are listed in Table 1. *Pta*6605 strains were maintained in King's B (KB) medium supplemented with 50 μg/ml nalidixic acid (Nal) at 27ºC (King et al. 1954; Taguchi et al. 2003). *E. coli* strains were grown in Luria Bertani (LB) medium supplemented with appropriate antibiotics at 37ºC.

Host plant and inoculation procedure

Tobacco plants used in this study (*Nicotiana tabacum* L. var. Xanthi NC) were grown at 28ºC with an 18-h photoperiod. Plant infection assays were carried out by several methods. We modified a flood inoculation system for tobacco seedlings based on the system that was described in Ishiga et al. (2011). Tobacco seeds were sterilized and sown on Murashige-Skoog (MS) 0.8% agar plates containing 1% sucrose and vitamin stock solution (thiamin hydrochloride 3 mg/L, nicotinic acid 5 mg/L, pyridoxine hydrochloride 0.5 mg/L), and grown at 28ºC under 16 h light-8 h dark conditions for 2 wk. Tobacco seedlings were transplanted to MS 0.8% agar plates containing 0.1% sucrose and vitamin stock solution as described above and grown for 2 d under the same conditions. Bacteria were grown overnight at 27ºC in LB medium with 10 mM $MgCl_2$. The bacterial inoculum was adjusted to OD_{600} = 0.004 (8×10^6

colony forming unit, (CFU)/ml) with sterilized 10 mM $MgSO_4$ containing 0.025% (v/v) Silwet L-77 (OSI Specialties, Danbury, CT). Sterilized 10 mM $MgSO_4$ was used as a mock inoculation. The bacterial suspension (approximately 30 ml) was poured onto the plate of tobacco seedlings. After about 10 sec incubation, the bacterial suspension was decanted, and the plate was air-dried on a clean bench for 15 min. The plants were incubated under 16 h light-8 h dark conditions at 22ºC and disease symptoms were observed for 3 d post-inoculation (dpi). To determine the bacterial population at 3 h post-inoculation (hpi) and 3 dpi, leaf disks were punched out using a disposable biopsy hole punch and then ground with a mortar and pestle. The homogenates were serially diluted in sterile distilled water and then spread on KB plates containing Nal. The plates were dried and incubated at 27ºC for 2 d, after which the bacterial population was measured by counting the number of colonies, CFU.

We also employed the classical dip inoculation method described by Taguchi and Ichinose (2011) with some modifications. A single colony of bacteria was grown in 3 mL LB with $MgCl_2$. After 8 h incubation at 27ºC, bacteria were re-inoculated into 10 mL KB medium without antibiotic and further incubated at 27ºC for 12–16 h. The bacteria suspension was then washed with 10 mM $MgSO_4$ and adjusted to OD_{600} of 0.1 (approximate density of bacteria was 2×10^8 CFU/mL). Silwet L-77 was added at 0.04% (v/v) to the bacterial suspension prior to the dip inoculation experiment. Detached leaves of 8-wk-old tobacco plants were dipped into the bacterial suspension for 2 min and placed in a tray covered with plastic wrap. Cut petioles were wrapped and supplied water with cotton. Pictures were taken 5 and 10 dpi. In one experiment, three leaves from independent plants were used for each bacterial strain.

The infiltration experiment was done by injecting bacterial cells with a needleless syringe at density 2 × 10^5 CFU/mL into attached leaves of whole plants or detached tobacco leaves (three leaves for each bacterial strain). The inoculated detached leaves and plants were incubated in a growth chamber at 22ºC with a long-day photoperiod (16 h light-8 h dark). Disease development was observed, and photographs were taken at 14 dpi.

Construction of *che* deletion mutant strains

To generate deletion mutant strains, genetic regions containing *cheA1* (A3SK_RS0109815), *cheY1* (A3SK_RS0109825), *cheA2* (A3SK_RS0105665), and *cheY2* (A3SK_RS0105655) in *Pta*6605 were amplified and subcloned into a pGEM®-T Easy Vector (Promega, Madison, WI, USA) by the respective primer pairs listed in Table 2. The next sets of primer pairs then were used to delete each open reading frame (ORF) by inverse PCR. This procedure resulted in the internal deletion of 2080 bp, 340 bp, 2270 bp, and 360 bp of *cheA1*, *cheY1*, *cheA2*, and *cheY2*, respectively (Fig. 1). PCR products were treated by *Dpn*I and digested by *Bam*HI, then self-ligated using 2 × Ligation mix (Nippon Gene, Tokyo, Japan). Each deletion mutant DNA fragment was excised and inserted into the mobilizable cloning vector pK18*mobsacB* via *Eco*RI site (Schäfer et al. 1994). The resulting plasmids were transformed into *E. coli* strain S17-1 and integrated into the wild-type (WT) strain of *Pta*6605 by conjugation and homologous recombination according to the previously described method (Shimizu et al. 2003; Ichinose et al. 2020). The sequence of each recombinant DNA was confirmed by DNA sequencing using a Big Dye Terminator Cycle Sequencing Kit and ABI PRISM 3100 sequencer (Thermo Fisher Scientific, Waltham, MA, USA).

Construction of complemented strains

To generate complemented strains of *cheA1*, *cheA2,* and *cheY2*, full lengths of each gene fragment with their predicted promoter regions were amplified using the primers listed in Table 2, and then cloned into expression vector pDSK519 (Keen et al. 1988) at *Bam*HI (*cheA2*), *Not*I (*cheY2*), and *Eco*RI (*cheA1*) sites. Recombinant plasmids were transformed into *E. coli* S17-1 and introduced into Δ*cheA2*, Δ*cheY2*, and Δ*cheA1* by conjugation.

Chemotaxis assay

Chemotaxis was assayed by a microtiter plate multi-capillaries method (Reyes-Darias et al. 2016) with minor modification. Bacteria were grown in 3 mL LB with 10 mM $MgCl_2$ overnight and inoculated into 3 mL fresh minimal medium supplemented with 10 mM of mannitol and fructose (MMMF, 50 mM potassium phosphate, 7.6 mM $(NH_4)_2SO_4$, 1.7 mM $MgCl_2$, 1.7 mM NaCl, and 10 mM mannitol and fructose) for further 5 h incubation. Then cells were washed twice with 10 mM HEPES buffer by 1700 × g centrifugation for 10 minutes at 25ºC. The cell density was adjusted to OD_{600} of 0.05 with 10 mM HEPES as chemotaxis buffer. To prepare the capillary for the chemotaxis assay, one end of a 5 µL capillary (Drummond Scientific Company, Broomall, PA, USA) was sealed with a flame. The heated capillary was dipped into 1% yeast extract or 10 mM HEPES buffer to fill it as negative control. A rubber collar was fitted onto the capillary to support it during the assay. Each well of the round-bottom Falcon® microtiter plate (Corning, Corning, NY, USA) was filled with 230 µL bacterial suspension and the prepared capillary was dipped into the bacterial suspension. After incubation for 30 minutes at 27ºC, the capillary was washed with sterile distilled water, and the contents of the capillary (5 µL) was squirted into 45 µL 0.9% NaCl. Following serial dilution, 10 µL of bacterial suspension was plated onto a KB plate containing 50 µg/ml Nal. The plate was incubated at

27ºC for 2 d, and the number of colonies that appeared was counted to determine the strength of chemotaxis.

Motility assay

Bacterial surface swarming and swimming motility tests were conducted as described previously (Taguchi and Ichinose 2011). Briefly, bacteria cultured overnight in 3 mL LB with 10 mM $MgCl_2$ were washed and resuspended in 10 mM $MgSO_4$ to an OD_{600} of 0.1. Three µL of bacterial suspension was spotted on the center of SWM plates (0.45% agar, 0.5% peptone, and 0.3% yeast extract; Difco, Detroit, MI, USA) for the swarming assay and 0.25% agar MMMF plates for the swimming assay. The swarming plate was incubated at 27ºC and photographed at 48 h after inoculation, while the swimming plate was incubated at 23ºC and was photographed at 72 h after inoculation.

Statistical analyses

The results of chemotaxis assays and measurements of bacterial growth are expressed as means with standard error. One-way/two-way ANOVA followed by Tukey's or Dunnett's highly significant difference tests were performed using GraphPad Prism ver. 8 (GraphPad Software Inc., San Diego, CA, USA). $P < 0.05$ was considered statistically significant.

Results

Identification of chemotaxis gene clusters in *P. syringae* pv. *tabaci* 6605

In a draft genome sequence of *Pta*6605, we found two chemotaxis gene clusters that include the genes encoding CheA and CheY proteins (Fig. 1). A phylogenetic tree of CheA was constructed (Fig. 2). The CheA2 of *P. syringae* belongs to the same clade as those of *P.*

aeruginosa (CheA1), *P. fluorescens* (CheA1), and *V. cholerae* (CheA2) which are known to be functional (Ferrández et al. 2002; Gosink et al. 2002; Manoharan et al. 2015; Muriel et al. 2015) (group III). It is known that there are plural *cheA* genes in the genome of the above species. Meanwhile, CheA1 of *P. syringae* is similar to other members of the CheA proteins such as *P. aeruginosa* (CheA2), *P. fluorescens* (CheA2 and CheA3), and *V. cholerae* (CheA3), and all members of group II belong to the same clade. We also observed that functional CheA proteins from *E. coli*, *R. solanacearum*, and *S. enterica* (Olsen et al. 2013; Parkinson 1978; Yao and Allen 2006) constructed a single clade, and each species has only single gene for *cheA* (group I). The remaining CheA, CheA1 of *V. choletrae*, showed low homology with other CheA proteins and comprised another independent clade (group IV).

Phylogenetic analysis of CheY amino acid sequences also showed four clades (Fig. S1). Interestingly, each CheY protein of the clade in Fig. S1 is a partner protein of CheA of the corresponding group (Fig. 2). For example, CheA1 of *Pto*DC3000 and *Pta*6605 and CheA2 of *P. aeruginosa* belong to group II (Fig. 2), and CheY1 of *Pto*DC3000, *Pta*6605, and CheY2 of *P. aeruginosa* also belong to group II (Fig. S1). Furthermore, CheA2 of *Pto*DC3000 and *Pta*6605 and CheA1 of *P. aeruginosa* belong to group III, and CheY2 of *Pto*DC3000 and *Pta*6605 and CheY1 of *P. aeruginosa* also belong to group III (Clarke et al. 2016; Ferrández et al. 2002). In the same way, CheA and CheY proteins of *S. enterica*, *E. coli*, and *R. solanacearum* belong to group I (Fig. 2 and Fig. S1, Kuo and Koshland 1987; Stecher et al. 2004), and the remaining CheA1, CheY1, and CheY2 of *V. cholerae* belong to group IV. In this paper, we used the names ‘group II chemotaxis gene cluster’ and ‘group III chemotaxis gene cluster’ to avoid confusion (Fig. 1, 2 and Fig. S1).

Surface motility of *cheA* and *cheY* deletion mutants

To investigate how CheA and CheY contribute to *Pta*6605 motility, we first conducted surface swarming assays. In liquid medium, both Δ*cheA2* and Δ*cheY2* mutants were still able to swim, but only in a 'running' mode. On the other hand, both Δ*cheA1* and Δ*cheY1* mutants were able to 'run' and 'tumble' just like WT (data not shown). In semi-solid media, however, some surface motilities were compromised. Surface swarming assays showed that Δ*cheA1* and Δ*cheY1* have swarming abilities similar to the WT strain, whereas the swarming ability of both Δ*cheA2* and Δ*cheY2* was lost (Fig. 3A). Complementation by introducing full length *cheA2* and *cheY2* to each respective mutant strain restored surface swarming motilities. The swimming motility of Δ*cheA2* and Δ*cheY2* was also lost, whereas that of Δ*cheA1* and Δ*cheY1* was reduced to some extent (Fig. 3B). Furthermore, complementation of *cheY2* in the Δ*cheY2* mutant restored some swimming motility, while the complementation of strain *cheA2* did not restore the phenotype (Fig. 3B).

Chemotaxis ability

Quantitative chemotaxis assays were conducted to investigate how the deletion of *cheA* and *cheY* genes on both clusters affect chemotaxis of *Pta*6605 to 1% yeast extract as a known attractant. Quantified results clearly showed that the chemotaxis of Δ*cheA1* and Δ*cheY1* was slightly reduced from the WT strain, whereas Δ*cheA2* and Δ*cheY2* had remarkably reduced chemotaxis, and both complemented strains restored the phenotype (Fig. 4). These indicated that the group III chemotaxis gene cluster (cluster II) is indispensable for *Pta*6605 chemotaxis, whereas mutation in the group II chemotaxis gene cluster (cluster I) has almost no effect.

Virulence of mutants on host tobacco leaves

The ability of the WT and *che* mutant strains to cause disease on host tobacco plants was investigated by a flood assay optimized for tobacco seedlings (Fig. 5), dip inoculation, and infiltration (Fig. 6). In the flood assay inoculation, Δ*cheA1*, Δ*cheA2*, and Δ*cheY2* were less virulent than the WT strain, whereas Δ*cheY1* was virulent, and complemented strains, Δ*cheA2*-C and Δ*cheY2*-C, restored the virulence although it was still weaker than that of the WT strain (Fig. 5A). We also investigated bacterial propagation in the seedling leaves (Fig. 5B) and found that both Δ*cheA2* and Δ*cheY2* mutants and Δ*cheA1* grew less than the WT strain at both time points, although the differences are not significant at 3 hpi, while Δ*cheY1* propagated to the same level as the WT strain. Both complemented strains, Δ*cheA2*-C and Δ*cheY2*-C, retained the same ability to propagate on host tobacco seedlings as the WT strain.

Dip inoculation with detached leaves showed that WT and Δ*cheY1* caused similar severe disease symptoms, and Δ*cheA1* also caused disease symptoms, although the severity of symptoms of Δ*cheA1* was weaker than those of WT and Δ*cheY1* (Fig. 6A). Furthermore, Δ*cheA2* did not cause any symptoms, and Δ*cheY2* caused very mild chlorosis and necrotic lesions. However, we observed that Δ*cheA1* was less virulent in the flood inoculation method (Fig. 5). We confirmed the reproducibility these results with different lines of Δ*cheA1* mutant strains and got the same results (Fig. S2A).

Differences in virulence of WT and mutant strains were also investigated by the infiltration inoculation method with attached leaves of whole plants. Although we speculated that mutation of the *che* genes would not have any effect when the bacteria were directly injected into the leaf's apoplastic spaces by infiltration, Δ*cheA1*, Δ*cheA2*, and Δ*cheY2* caused just few localized lesions, while WT and Δ*cheY1* caused the same level of disease symptoms

in the inoculated leaves of whole plants (Fig. 6B). The complemented strains, Δ*cheA2*-C and Δ*cheY2*-C, showed partially restored virulence. Because Δ*cheA1* showed different phenotypes between dip and infiltration inoculation (Fig. 6), we also performed infiltration inoculation using detached leaves and attached leaves of whole plants. As shown in Fig. S2C, all Δ*cheA1* strains did not cause any disease symptoms when we used whole plants, but developed disease symptoms like the WT strain on detached leaves.

To investigate the viability, all mutant strains were grown in liquid rich KB and MMMF media (Fig. S3). In rich KB medium, no mutant strain showed delayed logarithmic growth compared to WT. Instead, Δ*cheY1*, Δ*cheA2* and Δ*cheY2* mutants grew faster. However, in a minimal media that mimics the apoplastic space of plants, only Δ*cheA1* and Δ*cheY2* grew less than WT at most time points.

In *trans* complementation of *cheA1* does not restore Δ*cheA1* phenotypes

Δ*cheA1* had reduced swimming motility and lost virulence on host tobacco plants. To elucidate the reason behind the loss of phenotypes, we introduced the *cheA1* gene into the mutant strain. However, the complementation did not help the mutant strain to recover its swimming motility and virulence (Fig. S4).

Phenotypic assay of *cheY1*/*cheA1* overexpression on Δ*cheY2*/Δ*cheA2*

We also conducted experiments on overexpressing *cheY1* in Δ*cheY2* as well as *cheA1* in Δ*cheA2* to determine whether overexpression of *cheY1*/*cheA1* can replace *cheY2*/*cheA2* functions. Our results showed that overexpressing both *che1* genes did not complement the Δ*cheY2* and Δ***cheA2*** ability to swim and swarm on soft agar, and further the ability to infect tobacco seedlings (Fig. S5 and Fig. S6).

Discussions

Plant pathogenic bacteria employ various virulence factors for effective plant infection. Among the virulence factors including the well-characterized type III secretion system, motility of flagella and type IV pili, and phytotoxin production, chemotaxis is considered important for bacteria to navigate through the plant phylloplane toward signal cues coming from stomata or wounds (Ichinose et al. 2013; Matilla and Krell 2018). The versatility of chemotaxis in phytopathogenic bacteria can be understood from the large number of chemotaxis receptor genes compared to animal pathogenic bacteria: for example, *P. syringae* possesses about 50 genes for chemoreceptors, MCP, whereas *P. aeruginosa* possesses only 24–26 *mcp* genes (Matilla and Krell 2018). Furthermore, it is known that Pseudomonad bacteria possess plural chemotaxis gene clusters (Clarke et al. 2016; Ferrández et al. 2002; Muriel et al. 2015). In the beneficial strains like *P. fluorescens* F113, more than one chemotaxis system is necessary for rhizosphere colonization (Muriel et al. 2015). Such versatility makes the chemotaxis system difficult to characterize. In this study, we attempted to characterize the function of chemotaxis systems in a highly motile bacterium, *Pta*6605.

*Pta*6605 possesses two major chemotaxis systems

P. syringae shares high genomic DNA homology among its pathovars. The whole genome sequence of *Pto*DC3000 was previously determined (Buell et al. 2003), and it possesses *che1* (group II chemotaxis gene cluster) and *che2* (group III chemotaxis gene cluster) containing *cheA* and *cheY* for a two-component system and three minor chemotaxis gene clusters without *cheA* and *cheY* (Clarke et al. 2016). Because *cheA* and *cheY* are indispensable genes for

chemotaxis, we speculated that there are two major chemotaxis gene clusters.

The existence of multiple *che* clusters in the *P. syringae* genome indicates the complexity of the chemotaxis configuration. Like *Pto*DC3000, *Pta*6605 has group II and group III chemotaxis gene clusters containing *cheA* and *cheY,* demonstrating the importance of these two major chemotaxis gene clusters (Fig. 1). We compared *Pta*6605 CheA and CheY amino acid sequences with those of other Gram-negative bacteria and generated phylogenetic trees (Fig. 2 and Fig. S1). The effects of mutation in each *cheA* or *cheY* gene obtained from the previous reports and this study was incorporated into the phylogenetic trees as symbols. Interestingly, the *cheA* and *cheY* gene mutations that resulted in the remarkable reduction or loss of motility were concentrated in two respective clades, groups I and III; furthermore, mutation of *cheA* and *cheY* genes in the other clades, groups II and IV, only weakly reduced motility or had no effect. The group I bacteria such as *R. solanacearum*, *E. coli*, and *S. enterica* have only one *cheA* and *cheY*, while *Pseudomonas* and *Vibrio* species have plural sets of chemotaxis genes (groups II, III, and IV). Among them, *cheA* and *cheY* genes in group III seem to be essential and major, and those of group II and IV seem to be redundant. Therefore, the group III chemotaxis gene cluster in *Pta*6605 is the major chemotaxis gene cluster controlling the flagellar-based chemotaxis and motility. However, Δ*cheA1* showed less virulence than the WT strain in all inoculation methods (Fig. 5 and Fig. S2), indicating that CheA1 plays some role in plant–pathogenic bacteria interactions.

Group III chemotaxis gene cluster controls flagellar-based motility and chemotaxis of *Pta*6605

Swarming is a movement of coordinated multicellular flagellated bacteria across a solid surface (Kearns 2010). Unlike swarming, swimming motility is a movement of individual cells in a liquid environment and is associated with flagella rotation and chemotaxis (Wadhams and Armitage 2004). Previous studies reported that Δ*fliC* and Δ*motCD* mutants lost surface swarming and swimming motilities in a semisolid agar medium (Kanda et al. 2011; Shimizu et al. 2003; Taguchi et al. 2006), and the Δ*pilA* mutant lost surface swarming motility and had reduced swimming motility, although Δ*pilA* retained the swimming ability in a liquid medium (Taguchi and Ichinose 2011). These results demonstrated that surface motility is dependent on bacterial flagella and pili, and are consistent with our finding that Δ*cheA2* and Δ*cheY2* had lost surface swarming motility (Fig. 3A) and had remarkably reduced chemotaxis to 1% yeast extract (Fig. 4). Furthermore, the swimming ability of Δ*cheA2* and Δ*cheY2* was completely abolished on MMMF semisolid media (Fig. 3B), therefore implying that the group III chemotaxis gene cluster is the canonical chemotaxis pathway responsible for flagellar-mediated motility and chemotaxis. In *P. aeruginosa*, the PAO1 mutation of genes located in the group III chemotaxis gene cluster also resulted in the loss of chemotactic motility (Ferrández et al. 2002; Güvener et al. 2006).

However, the function of the group II chemotaxis gene cluster is still unclear. Although these genes were not necessary for surface swarming motility and chemotaxis in *Pta*6605, the *cheA1* mutant had reduced swimming motility and was less virulent in the flood inoculation method (Fig. 5A & S2A) and infiltration of attached leaves (Fig. S2C). The partially similar results were obtained by Clarke et al. (2016), using a *cheA* mutant of *Pto*DC3000, in which *cheA1* retained swimming and swarming motilities but reduced virulence on its host

tomato plant. Unexpectedly, the complemented strain of *cheA1* mutant that we generated did not restore the swimming motility and virulence (Fig. S4). This might be due to polar effects that occurred during mutagenesis, and the complemented strain might have a defect in the gene expression of the group II chemotaxis gene cluster because this region is known to be important for chemotaxis and signal transduction. For example, *mcpB*, which localizes downstream of *cheA2* in PAO1 is possibly essential for signal transduction (Güvener et al. 2006), and mutation of *cheB2* reduced chemotaxis (Ferrández et al. 2002).

Group III chemotaxis gene cluster may modulate not only chemotaxis functions but also other virulence factors

Virulence assays were done to further investigate how necessary motility and chemotaxis are for *Pta*6605 to cause disease in host plants. The flood assay inoculation (Fig. 5) which mimics the condition in nature provided the idea that *cheA2* and *cheY2* mutants that are impaired in motility and chemotaxis are unable to enter and colonize the apoplastic space and thus fail to cause disease. These data are also consistent with those reported by Clarke et al. (2016). Clarke et al. found that *cheA2* mutants of *Pto*DC3000 and another strain *Pto*1108 propagated less in host plants, indicating that the motility and chemotaxis dominated by group III chemotaxis gene cluster are primarily important during the early stage of infection. However, following dip inoculation, *cheA1* and *cheY1* may not be needed for *Pta*6605 virulence (Fig. 6A). This might be because a detached leaf does not have the optimal defense against infection that seedlings have.

We also inoculated tobacco leaves of whole plants by infiltration (Fig. 6B). Contrary

to the previous beliefs that motility and chemotaxis are not important once bacteria enter a favorable infection site (Clarke et al. 2016; Yu et al. 2013), Δ*cheA2*, Δ*cheY2*, and even Δ*cheA1* had decreased ability to cause disease in infiltration inoculation (Fig. 6B). These results indicate that beside chemotactic motility, *cheA2* and *cheY2* may regulate another signal transduction pathway. Recently, Cerna-Vargas et al. (2019) also reported that the amino acid chemoreceptor, PscA of *Pto*DC3000 mediates not only chemotaxis but also controls the level of cyclic di-GMP, biofilm formation, and swarming motility through perception of the abundant plant amino acids. The chemotactic signaling pathway may affect not only directional motility but also the expression of various virulence-related genes. Furthermore, the virulence of Δ*cheA1* differed depending on the inoculation method: a moderate level of disease symptoms was developed by the dip inoculation method (Fig. 6A), whereas no symptoms appeared with flood and infiltration inoculation methods (Fig. 5 and Fig. 6B). Because the dip inoculation method uses detached leaves, whereas flood and infiltration inoculation methods use whole plants, we performed infiltration experiments using detached leaves and leaves of whole plants (Fig. S2). The Δ*cheA1* caused WT level disease symptoms in detached leaves, whereas it did not cause any symptoms in whole plants, suggesting that a weakened defense system in detached leaves allowed the successful Δ*cheA1* invasion. We also cannot rule out the possibility of Δ*cheA1* bacterial viability inside the attached leaves because of its slower growth in minimal media (Fig. S3). However, a complemented strain of the *cheA1* mutant did not recover virulence by infiltration and flood assay inoculation method (Fig. 6B and Fig. S4B), as discussed above. Further, these results indicate that *cheA1* also necessary for *Pta*6605 to cause disease on host tobacco plants.

Overexpression of *cheY1* in the Δ*cheY2* and *cheA1* in the Δ*cheA2* did not change the phenotypes (Fig. S5 and Fig. S6), unlike overexpression of *cheB2* in the Δ*cheB* mutant of PAO1, which was able to partially complement the phenotype (Ferrández et al. 2002). Possessing multiple chemotaxis cluster indicating the complexity of *Pta*6605 chemotaxis system. There have been discussions about the relation between the localization of chemotaxis protein and their functions in *Rhodobacter sphaeroides* and *E. coli* (Sourjik and Armitage 2010). Deletion of a chemotaxis gene cannot be complemented by expressing its homologs from different chemotaxis gene clusters because one of them is localized in cell pole while the another is cytoplasmic. This result suggests that the roles of CheY1/CheA1 and CheY2/CheA2 in the *Pta*6605 chemotaxis signaling pathway and their localization are not identical, thus CheY1/CheA1 is not able to substitute the loss of CheY2/CheA2.

Some reports have described how chemotaxis systems are correlated with other functions beside chemotaxis, such as cholera toxin production in *V. cholera* (Bandyopadhaya and Chaudhuri 2009; Lee et al. 2001). As discussed above, the ability of CheA2 to phosphorylate other CheYs opens the possibility that *Pta*6605 CheA2 may regulate many bacterial functions other than chemotaxis (Porter and Armitage 2002; Szurmant and Ordal 2004). Several characterizations of relevant virulence factors and gene expression analysis in *Pta*6605 are needed to support this idea. Nevertheless, considering all the inoculation results, we propose that the group III chemotaxis gene cluster in *Pta*6605 might function as a major part of the complex virulence regulators, and is thus required for fully functional chemotaxis and optimal host infection.

Acknowledgements

The first author was supported by the Japanese Government through a MONBUKAGAKUSHO (MEXT) Scholarship during her study at Okayama University. The *Pseudomonas syringae* pv. *tabaci* 6605 isolate was kindly provided by the Leaf Tobacco Research Laboratory of Japan Tobacco Inc. We thank Prof. J. Kato and Dr. S. Oku, Hiroshima University, for the technical advice on the chemotaxis test. This work was supported in part by Grants-in-Aid for Scientific Research (Nos. 26660035 and 19H02956) from the Ministry of Education, Culture, Sports, Science and Technology of Japan.

Compliance with ethical standards

Conflict of interest

All authors declare that there is no conflict of interest.

Ethical approval

This article does not include any experiments with animals or human conducted by any of the authors.

References

Antunnez-Lamaz, M, Cabrera E, Lopez-Solanina E, Solano R, González-Melendi P, Chico JM, Toth I, Birch P, Prichard L, Liu H, Rodriguez- Palenzuela P (2009) Bacterial chemoattraction towards jasmonate plays a role in the entry of *Dickeya dadantii* through wounded tissues. Mol Microbiol 74:662-671.

Bandyopadhaya A, Chauduri K (2009) Differential modulation of NF-κB-mediated pro-inflammatory response in human intestinal epithelial cells by cheY homologues of *Vibrio cholerae*. Innate Immun 15: 131-142.

Bi S, Lai L (2015) Bacterial chemoreceptors and chemoeffectors. Cell Mol Life Sci 72:691-708.

Blair DF (1995) How bacteria sense and swim. Annu Rev Microbiol 49:489-522.

Blattner FR, Plunkett G, Bloch CA, Perna NT, Burland V, Riley M, Collado-Vides J, Glasner JD, Rode CK, Mayhew GF, Gregor J, Davis NW, Kirkpatrick HA, Goeden MA, Rose DJ, Mau B, Shao Y (1997) The complete genome sequence of *Escherichia coli* K-12. Science 277:1453–1462.

Buell CR, Joardar V, Lindeberg M, Selengut J, Paulsen IT, Gwinn ML, Dodson RJ, Deboy RT, Durkin AS, Kolonay JF, Madupu R, Daugherty S, Brinkac L, Beanan MJ, Haft DH, Nelson WC, Davidsen T, Zafar N, Zhou L, Liu J, Yuan Q, Khouri H, Fedorova N, Tran B, Russel D, Berry K, Utterback T, Van Aken SE, Feldblyum TV, D'Ascenzo M, Deng WL, Ramos AR, Alfano JR, Cartinhour S, Chatterjee AK, Delaney TP, Lazarowitz SG, Martin GB, Schneider DJ, Tang X, Bender CL, White O, Fraser CM, Colmer A (2003) The complete genome sequence of the *Arabidopsis* and tomato pathogen *Pseudomonas syringae* pv. tomato DC3000. Proc Natl Acad Sci USA 100:10181-10186.

Cerna-Vargas JP, Santamaría-Hernando S, Matilla MA, Rodríguez-Herva JJ, Daddaoua A, Rodríguez-Palenzuela P, Krell T, López-Solanilla E (2019) Chemoperception of specific amino acids controls phytopathogenicity in *Pseudomonas syringae* pv. tomato. mBio 10, e01868-19.

1 Clarke CR, Hayes BW, Runde BJ, Markel E, Swingle BM, Vinatzer BA (2016) Comparative
2 genomics of *Pseudomonas syringae* pathovar *tomato* reveals novel chemotaxis pathway
3 associated with motility and plant pathogenicity. PeerJ 4:e2570.
4 Feng L, Reeves PR, Lan R, Ren Y, Gao C, Zhou Z, Ren Y, Cheng J, Wang W, Wang J, Qian
5 W, Li D, Wang L (2008) A recalibrated molecular clock and independent origins for the
6 cholera pandemic clones. PLoS One 3:e4053.
7 Ferrández A, Hawkins AC, Summerfield DT, Harwood CS (2002) Cluster II *che* genes from
8 *Pseudomonas aeruginosa* are required for an optimal chemotactic response. J Bacteriol
9 184:4374-4383.
10 Gosink KK, Kobayashi R, Kawagishi I, Häse CC (2002) Analyses of the roles of the three
11 cheA homologs in chemotaxis of *Vibrio cholerae*. J Bacteriol 184: 1767-1771.
12 Güvener ZT, Tifrea DF, Harwood CS (2006) Two different *Pseudomonas aeruginosa*
13 chemosensory signal transduction complexes localize to cell poles and form and remould
14 in stationary phase. Mol Microbiol 61:106-118.
15 Ichinose Y, Shimizu R, Ikeda Y, Taguchi F, Marutani M, Mukaihara T, Inagaki Y, Toyoda K,
16 Shiraishi T (2003) Need for flagella for complete virulence of *Pseudomonas syringae* pv.
17 *tabaci*: genetic analysis with flagella-defective mutants Δ*fliC* and Δ*fliD* in host tobacco
18 plants. J Gen Plant Pathol 69:244-249.
19 Ichinose Y, Taguchi F, Mukaihara T (2013) Pathogenicity and virulence factors of
20 *Pseudomonas syringae*. J Gen Plant Pathol 79:285-296.
21 Ichinose Y, Tasaka Y, Yamamoto S, Inoue Y, Takata M, Nakatsu Y, Taguchi F, Yamamoto
22 M, Toyoda K, Noutoshi Y, Matsui H (2020) PsyR, a transcriptional regulator in quorum

sensing system, binds *lux* box-like sequence in *psyI* promoter without AHL quorum sensing molecule and activates *psyI* transcription with AHL in *Pseudomonas syringae* pv. *tabaci* 6605. J Gen Plant Pathol 86:124-133.

Ishiga Y, Ishiga T, Uppalapati SR, Mysore KS (2011) Arabidopsis seedling flood-inoculation technique: a rapid and reliable assay for studying plant-bacterial interactions. Plant Methods 7: 32.

Joardar V, Lindeberg M, Jackson RW, Selengut J, Dodson R, Brinkac LM, Daugherty SC, Deboy R, Durkin AS, Giglio MG, Madupu R, Nelson WC, Rosovitz MJ, Sullivan S, Crabtree J, Creasy T, Davidsen T, Haft DH, Zafar N, Zhou L, Halpin R, Holley T, Khouri H, Feldblyum T, White O, Fraser CM, Chatterjee AK, Cartinhour S, Schneider DJ, Mansfield J, Collmer A, Buell CR (2005) Whole-genome sequence analysis of *Pseudomonas syringae pv. phaseolicola* 1448A reveals divergence among pathovars in genes involved in virulence and transposition. J Bacteriol 187:6488–6498.

Kanda E, Tatsuta T, Suzuki T, Taguchi F, Naito K, Inagaki Y, Toyoda K, Shiraishi T, Ichinose Y (2011) Two flagellar stators and their roles in motility and virulence in *Pseudomonas syringae* pv *tabaci* 6605. Mol Genet Genomics 285:163-174.

Kato J, Nakamura T, Kuroda A, Ohtake H (1999) Cloning and characterization of chemotaxis genes in *Pseudomonas aeruginosa*. Biosci Biotechnol Biochem 63:155-161.

Kearns DB (2010) A field guide to bacterial swarming motility. Nat Rev Microbiol 8:634-644.

Keen NT, Tamaki S, Kobayashi D, Trollinger D (1988) Improved broad-host-range plasmids for DNA cloning in Gram-negative bacteria. Gene 70:191-197.

King EO, Ward MK, Raney DE (1954) Two simple media for demonstration of pyocyanin and fluorescein. Transl Res 44:301-307.

Kroupitski Y, Goldberg D, Belausoy E, Pinto R, Swartzberg D, Granot D, Sela S (2009) Internalization of *Salmonella enterica* in leaves is induced by light and involves chemotaxis and penetration through open stomata. Appl Environ Microbiol 75:6076-6086.

Kuo SC, Koshland DE (1987) Roles of *cheY* and *cheZ* gene products in controlling flagellar rotation in bacterial chemotaxis of *Escherichia coli*. J Bacteriol 169:1307-1314.

Lee SH, Butler SM, Camilli A (2001) Selection for *in vivo* regulators of bacterial virulence. Proc Natl Acad Sci USA 98:6889-6894.

Manoharan B, Neale HC, Hancock JT, Jackson RW, Arnold DL (2015) The identification of genes important in *Pseudomonas syringae* pv. *phaseolicola* plant colonisation using in vitro screening of transposon libraries. PLoS One 10:1-19. e0137355.

Manson MD (1992) Bacterial motility and chemotaxis, in: Rose AH (Ed.), Advances in Microbial Physiology, Academic Press, New York, NY, pp. 277-346.

Matilla MA, Krell T (2018) The effect of bacterial chemotaxis on host infection and pathogenicity. FEMS Microbiol Rev 42:40-67.

McClelland M, Sanderson KE, Spieth J, Clifton SW, Latreille P, Courtney L, Porwollik S, Ali J, Dante M, Du F, Hou S, Layman D, Leonard S, Nguyen C, Scott K, Holmes A, Grewal N, Mulvaney E, Ryan E, Sun H, Florea L, Webb M, Stoneking T, Nhan M, Waterson R, Wilson RK (2001) Complete genome sequence of *Salmonella enterica* serovar Typhimurium LT2. Nature 413:852-856.

Melotto M, Underwood W, Koczan J, Nomura K, He SY (2006) Plant stomata function in innate immunity against bacterial invasion. Cell 126:969-980.

Muriel C, Jalvo B, Redondo-Nieto M, Rivilla R, Martin M (2015) Chemotactic motility of *Pseudomonas fluorescens* F113 under aerobic and denitrification conditions. PLoS ONE 10:1-13.

Olsen JE, Hoegh-Andersen KH, Casadesús J, Rosenkrantz JT, Chadfield MS, Thomsen LE (2013) The role of flagella and chemotaxis genes in host pathogen interaction of the host adapted *Salmonella enterica* serovar Dublin compared to the broad host range serovar *S.* Typhimurium. BMC Microbiol 13:67.

Parkinson JS (1978) Complementation analysis and deletion mapping of *Escherichia coli* mutants defective in chemotaxis. J Bacteriol 135:45-53.

Porter SL, Armitage JP (2002) Phosphotransfer in *Rhodobacter sphaeroides* chemotaxis. J Mol Biol 324:35-45.

Redondo-Nieto M, Barret M, Morrisey JP, Germaine K, Martinez-Granero F, Barahona E, Navazo A, Sánchez-Contreras M, Moynihan JA, Giddens SR, Coppoolse ER, Muriel C, Stiekema WJ, Rainey PB, Dowling D, O'Gara F, Martin M, Rivilla R (2011) Genome sequence of the biocontrol strain *Pseudomonas fluorescens* F113. J Bacteriol 194:1273-1274.

Reyes-Darias JA, Garcia V, Rico-Jiménez M, Corral-Lugo A, Krell, T (2016) Identification and characterization of bacterial chemoreceptors using quantitative capillary and gradient plate chemotaxis assays. Bio Protoc 6: e1789.

1 Salanoubat M, Genin S, Artiguenave F, Gouzy J, Mangenot S, Arlat M, Billault A, Brottier P,
2 Camus JC, Cattolico L, Chandler M, Choisne N, Claudel-Renard C, Cunnac S, Demange
3 N, Gaspin C, Lavie M, Moisan A, Robert C, Saurin W, Schiex T, Siguier P, Thébault P,
4 Whalen M, Wincker P, Levy M, Weissenbach J, Boucher CA (2002) Genome sequence
5 of the plant pathogen *Ralstonia solanacearum*. Nature 415:497-502.
6 Schäfer A, Tauch A, Jäger W, Kalinowski J, Thierbach G, Pühler A (1994) Small mobilizable
7 multi-purpose cloning vectors derived from the *Escherichia coli* plasmids pK18 and
8 pK19: selection of defined deletions in the chromosome of *Corynebacterium glutamicum*.
9 Gene 145:69-73.
10 Shimizu R, Taguchi F, Marutani M, Mukaihara T, Inagaki Y, Toyoda K, Shiraishi T, Ichinose
11 Y (2003) The DeltafliD mutant of *Pseudomonas syringae* pv, *tabaci*, which secretes
12 flagellin monomers, induces a strong hypersensitive reaction (HR) in non-host tomato
13 cells. Mol Genet Genomics 269:21-30.
14 Sourjik V, Armitage JP (2010) Spatial organization in bacterial chemotaxis. EMBO J 29:2724-
15 2733.
16 Sourjik V, Wingreen NS (2012) Responding to chemical gradients: bacterial chemotaxis. Curr
17 Opin Cell Biol 24:262-268.
18 Stecher B, Hapfelmeier S, Müller C, Kremer M, Stallmach T, Hardt WD (2004) Flagella and
19 chemotaxis are required for efficient induction of *Salmonella enterica* serovar
20 Typhimurium colitis in Streptomycin-pretreated mice. Infec Immun 72: 4138-4150.
21 Stover CK, Pham XQ, Erwin AL, Mizoguchi SD, Warrener P, Hickey MJ, Brinkman FSL,
22 Hufnagle WO, Kowalik DJ, Lagrou M, Garber RL, Goltry L, Tolentino E, Clarke et al.

(2016), PeerJ, DOI 10.7717/peerj.2570 23/24 Westbrock-Wadman S, Yuan Y, Brody LL, Coulter SN, Folger KR, Kas A, Larbig K, Lim R, Smith K, Spencer D, Wong GKS, Wu Z, Paulsen IT, Reizer J, Saier MH, Hancock REW, Lory S, Olson MV (2000) Complete genome sequence of *Pseudomonas aeruginosa* PAO1, an opportunistic pathogen. Nature 406:959-964.

Szurmant H, Ordal GW (2004) Diversity on chemotaxis mechanisms among the bacteria and archaea. Microbiol Mol Biol Rev 68:310-319.

Taguchi F, Takeuchi K, Katoh E, Murata K, Suzuki T, Marutani M, Kawasaki T, Eguchi M, Katoh S, Kaku H, Yasuda C, Inagaki Y, Toyoda K, Shiraishi T, Ichinose Y (2006) Identification of glycosylation genes and glycosylated amino acids of flagellin in *Pseudomonas syringae* pv. *tabaci*. Cell Microbiol 8:923-938.

Taguchi F, Yamamoto M, Ohnishi-Kameyama M, Iwaki M, Yoshida M, Ishii T, Konishi T, Ichinose Y (2010) Defects in flagellin glycosylation affect the virulence of *Pseudomonas syringae* pv. *tabaci* 6605. Microbiology 156:72-80.

Taguchi F, Ichinose Y (2011) Role of type IV pili in virulence of *Pseudomonas syringae* pv. *tabaci* 6605: correlation of motility, multidrug resistance, and HR-inducing activity on a non-host plant. Mol Plant Microbe Interact 24:1001-1011.

Wadhams GH, Armitage JP (2004) Making sense of it all: bacterial chemotaxis. Nat Rev Mol Cell Biol 5: 1024-1037.

Yao J, Allen C (2006) Chemotaxis is required for virulence and competitive fitness of the bacterial wilt pathogen *Ralstonia solanacearum*. J Bacteriol 188:3697-3708.

Yu X, Lund SP, Scott RA, Greenwald JW, Records AH, Nettleton D, Lindow SE, Gross DC, Beattie GA (2013) Transcriptional responses of *Pseudomonas syringae* to growth in epiphytic versus apoplastic leaf sites. Proc Natl Acad Sci USA 110:e425-e434.

Xin XF, Kvitko B, He SY (2018) *Pseudomonas syringae*: what it takes to be a pathogen. Nat Rev Microbiol 16:316-328.

Figure legends

Fig. 1 Chemotaxis gene clusters in *P. syringae* pv. *tomato* (*Pto*) DC3000, pv. *tabaci* (*Pta*) 6605 and *P. aeruginosa* (*Pa*) PAO1. Schematic organization of group II chemotaxis gene clusters including cluster I in *Pto*DC3000 and *Pta*6605, and cluster II in *Pa*PAO1 (**A**), and group III chemotaxis gene clusters including cluster II in *Pto*DC3000 and *Pta*6605, and cluster I in *Pa*PAO1 (**B**). The constructions of the Δ*cheA1*, Δ*cheY1*, Δ*cheA2*, and Δ*cheY2* mutants are also illustrated in *Pta* 6605. Light gray arrowheads indicate the positions of the PCR primers used to clone each *cheA* and *cheY* gene. Each gene name is shown in or above the pentagons. Inverse PCR was carried out to generate ORF-deleted DNA in each gene using primers indicated by dark gray arrowheads. Each ortholog is connected with shadow background.

Fig. 2 Phylogenetic tree comparing CheA protein sequences. A neighbor-joining tree based on aligned CheA protein sequences of *Pta*6605, *Pto*DC3000, *Pph*1448A, *R. solanacearum* GMI1000, *P. aeruginosa* PAO1, *E. coli* K-12, *P. fluorescens* F113, *V. cholerae* O395, and *S. enterica* serovar *typhimurium* LT2. Numbers at nodes represent bootstrap support based on 1000 replicates. Evolutionary distances were determined using the Poisson correction method

and are in units of the number of amino acid substitutions per site. The tree was generated using MEGA7 software. Circle marks indicate that mutation of *cheA* resulted in lost (black), reduced (gray), or unaffected (white) chemotaxis-related phenotypes. Each reference is also shown on the right.

Fig. 3 Surface motility phenotypes of WT and each mutant. (**A**) Surface swarming assay on SWM plates with 0.45% agar at 27ºC and (**B**) swimming assay on MMMF plates with 0.25% agar at 27ºC. Three µl of each bacterial suspension (2×10^8 CFU/ml) was spotted on the center of the plate and incubated for 48 h (swarming) and 72 h (swimming). The photographs show representative results obtained from three independent experiments (each with 2 technical replicates).

Fig. 4 Quantitative capillary chemotaxis assay of WT and each mutant to 1% yeast extract. The number of bacteria attracted into the capillary was measured in each strain. The experiment was repeated two times with two different colonies of each mutant, and similar results were obtained. Asterisks indicate statistically significant differences between WT and mutant strains (*P <0.05; **P <0.01; ***P <0.001; by Dunnett's multiple comparisons test). Error bars represent standard errors from two independent experiments (each with three technical replicates).

Fig. 5 Inoculation of host tobacco leaves by flood assay method. (**A**) Tobacco seedlings were inoculated by flooding with 8×10^6 CFU/ml bacterial suspension of each strain and incubated

at 22ºC. Photographs taken 3 and 8 dpi show representative results from three independent experiments. (**B**) Bacterial populations were counted at 3 hpi and 3 dpi. The bars represent the standard error from two independent experiments. Bacterial CFUs for each strain in one experiment were pooled from 3 (3 hpi) or 4 (3 dpi) individuals. Asterisks indicate statistically significant differences between WT and mutants (ns: not significant; $**P < 0.01$; $***P < 0.001$ by Dunnett's multiple comparisons test).

Fig. 6 Dip and infiltration inoculation tests on host tobacco leaves of the WT and each mutant. (**A**) Detached tobacco leaves were inoculated by dipping into 2×10^8 CFU/ml bacterial suspension of each strain and incubated at 22ºC. Photographs taken 5 and 10 dpi show representative results from three independent experiments. (**B**) Attached tobacco leaves of whole plants were infiltrated by 2×10^5 CFU/ml of each strain incubated at 22ºC. Photographs taken 14 dpi show representative results from two independent experiments. In one experiment, three leaves from independent plants were used for each bacterial strain.

Fig. S1 Phylogenetic tree comparing CheY protein sequences. A neighbor-joining tree based on aligned CheY protein sequences in *Pta*6605, *Pto*DC3000, *Pph*1448A, *R. solanacearum* GMI1000, *P. aeruginosa* PAO1, *E. coli* K-12, *P. fluorescens* F113, *V. cholerae* O395, and *S. enterica* serovar *typhimurium* LT2. Numbers at nodes represent bootstrap support based on 1000 replicates. Evolutionary distances were determined using the Poisson correction method and are in units of the number of amino acid substitutions per site. The tree was generated using MEGA7 software. A circle mark indicates that mutation of *cheY* resulted in

lost (black), reduced (gray), or unaffected (white) chemotaxis-related phenotype. Each reference is also shown on the right.

Fig. S2 Flood assay and infiltration inoculation tests on host tobacco plants (whole plants and detached leaves) of the WT and Δ*cheA1*. (**A**) Tobacco seedlings were inoculated by flooding with 8×10^6 CFU/ml bacterial suspension of each strain and incubated at 22ºC. Photographs taken 3, 5, and 9 dpi show representative results from two independent experiments. **(B)** Bacterial populations were counted at 3 hpi and 3 dpi. The bars represent standard error from two independent experiments. Bacterial CFUs for each strain in one experiment were pooled from 3 (3 hpi) or 4 (3 dpi) individuals. Asterisks indicate statistically significant differences between WT and mutants (ns: not significant; ***$P < 0.001$ by Dunnett's multiple comparisons test). **(C)** Tobacco leaves were infiltrated by 2×10^5 CFU/ml of each strain and incubated at 22ºC. Photographs taken 14 dpi show representative results from two independent experiments. In each experiment, two leaves from two independent plants were used.

Fig. S3 Growth curves of *P. syringae* pv. *tabaci* 6605 WT and its *che* mutant strains in (A) King's B medium and (B) MMMF medium. Bacterial growth was measured at OD_{595}. Asterisks indicate statistically significant differences between WT and mutants (ns: not significant; *P <0.05; **P <0.01; ***P <0.001 by Dunnett's multiple comparisons test). Data are means of two independent experiments conducted in triplicate.

Fig. S4 Swimming motility and virulence of Δ*cheA1* and its complemented strain. (**A**) Swimming motility on MMMF plates with 0.25% agar at 27ºC. Three µl of each bacterial suspension (2×10^8 CFU/ml) was spotted on the center of the plate and incubated for 72 h. The photographs show representative results obtained from two independent experiments (each with 3 technical replicates). (**B**) Flood assay inoculation. Tobacco seedlings were inoculated by flooding with 8×10^6 CFU/ml bacterial suspension of each strain and incubated at 22ºC. Photographs taken 3, 5, and 7 dpi show representative results from two independent experiments. **(C)** Bacterial populations were counted at 3 hpi and 3 dpi. The bars represent standard error from two independent experiments. Bacterial CFUs for each strain in one experiment were pooled from 3 (3 hpi) or 4 (3 dpi) individuals. Asterisks indicate statistically significant differences between WT and other tested strains (***$P < 0.001$ by Dunnett's multiple comparisons test). **(D)** Tobacco leaves were infiltrated by 2×10^5 CFU/ml of each strain and incubated at 22ºC. Photographs taken 10 dpi show representative results from two independent experiments. In one experiment, three leaves from three independent plants were used. "C" denotes Δ*cheA1* mutant complemented with *cheA1*.

Fig. S5 Effect of overexpression of *cheY1* in Δ*cheY2* mutant. (A) Swimming (MMMF plates with 0.25% agar) and swarming motilities (SWM plates with 0.45% agar) at 27ºC. Three µl of each bacterial suspension (2×10^8 CFU/ml) was spotted on the center of the plate and incubated for 72 h (swim) and 48 h (swarm). The photographs show representative results obtained from two independent experiments (each with 3 technical replicates). **(B)** Flood assay inoculation. Tobacco seedlings were inoculated by flooding with 8×10^6 CFU/ml bacterial suspension of

each strain and incubated at 22ºC. Photographs taken 3, 6, and 9 dpi show representative results from two independent experiments. **(C)** Bacterial populations were counted at 3 hpi and 3 dpi. The bars represent standard error from two independent experiments. Bacterial CFUs for each strain in one experiment were pooled from 3 (3 hpi) or 4 (3 dpi) individuals. Asterisks indicate statistically significant differences between WT and other tested strains (***$P < 0.001$ by Dunnett's multiple comparisons test). **(D)** Tobacco leaves were infiltrated by 2×10^5 CFU/ml of each strain and incubated at 22ºC. Photographs taken 10 dpi show representative results from two independent experiments. In one experiment, three leaves from three independent plants were used. "C" denotes Δ*cheY2* mutant complemented with *cheY1*.

Fig. S6 Effect of *cheA1* overexpression in *cheA2* mutant. (A) Swimming (MMMF plates with 0.25% agar) and swarming motilities (SWM plates with 0.45% agar) at 27ºC. Three µl of each bacterial suspension (2×10^8 CFU/ml) was spotted on the center of the plate and incubated for 72 h (swim) and 48 h (swarm). The photographs show representative results obtained from two independent experiments (each with 3 technical replicates). **(B)** Flood assay inoculation. Tobacco seedlings were inoculated by flooding with 8×10^6 CFU/ml bacterial suspension of each strain and incubated at 22ºC. Photographs taken 3, 6 and 9 dpi show representative results from two independent experiments. **(C)** Bacterial populations were counted at 3 hpi and 3 dpi. The bars represent standard error from two independent experiments. Bacterial CFUs for each strain in one experiment were pooled from 3 (3 hpi) or 4 (3 dpi) individuals. Asterisks indicate statistically significant differences between WT and other tested strains (***$P < 0.001$ by Dunnett's multiple comparisons test). **(D)** Tobacco leaves were infiltrated by 2×10^5 CFU/ml

of each strain and incubated at 22ºC. Photographs taken 10 dpi show representative results from two independent experiments. In one experiment, three leaves from three independent plants were used. "C" denotes Δ*cheA2* mutant complemented with *cheA1*.

Table 1 Plasmids used in this study for DNA cloning, mutant, and complement strain construction

Bacterial strain, plasmid	Relevant characteristics	Reference or source
Escherichia coli		
DH5α	*F– λ– ϕ80dLacZ ΔM15 Δ (lacZYA-argF)U169 recA1 endA1 hsdR17(rK – mK +) supE44 thi-1 gyrA relA1*	Nippon Gene, Tokyo, Japan
S17-1	*thi pro hsdR hsdR hsdM+ recA(chr::RP4-2-Tc::Mu-Km::Tn7)*	Schäfer *et al*. 1994
Pseudomonas syringae pv. *tabaci*		
Isolate 6605	Wild-type isolated from tobacco, Nal^r	Shimizu *et al*. 2003
6605-Δ*cheA1*	Isolate 6605 Δ*cheA1,* Nal^r	This study
6605-Δ*cheY1*	Isolate 6605 Δ*cheY1*, Nal^r	This study
6605-Δ*cheA2*	Isolate 6605 Δ*cheA2*, Nal^r	This study
6605-Δ*cheY2*	Isolate 6605 Δ*cheY2*, Nal^r	This study
6605-Δ*cheA2-C*	pD-*cheA2* containing Δ*cheA2*, Nal^r Km^r	This study
6605-Δ*cheY2-C*	pD-*cheY2* containing Δ*cheY2*, Nal^r Km^r	This study
6605- Δ*cheA1-C*	pD-*cheA1* containing Δ*cheA1*, Nal^r Km^r	This study
6605- Δ*cheY2-C (Y1)*	pD-*cheY1* containing Δ*cheY2*, Nal^r Km^r	This study
6605- Δ*cheA2-C (A1)*	pD-*cheA1* containing Δ*cheA2*, Nal^r Km^r	This study
Plasmid		
pGEM-TEasy	Cloning vector, Amp^r	Promega, Madison, WI, USA
pG-*cheA1*	*cheA1* fragment-containing pGEM-TEasy, Amp^r	This study
pG-*cheY1*	*cheY1* fragment-containing pGEM-TEasy, Amp^r	This study
pG-*cheA2*	*cheA2* fragment-containing pGEM-TEasy, Amp^r	This study
pG-*cheY2*	*cheY2* fragment-containing pGEM-TEasy, Amp^r	This study
pG-*pro-cheA2*	*cheA2* and its predicted promoter fragment-containing pGEM-TEasy, Amp^r	This study
pG-*pro-cheY2*	*cheY2* and its predicted promoter fragment-containing pGEM-TEasy, Amp^r	This study
pG-*pro-cheA1*	*cheA1* and its predicted promoter fragment-containing pGEM-TEasy, Amp^r	This study
pG-*pro-cheY1*	*cheY1* and its predicted promoter fragment-containing pGEM-TEasy, Amp^r	This study
pK18*mob*Sac*B*	Small mobilizable vector, Km^r, sucrose sensitive (s*acB*)	Schäfer *et al*. 1994
pK18- Δ*cheA1*	*cheA1* deleted DNA-containing pK18*mobsacB*, Km^r	This study
pK18- Δ*cheY1*	*cheY1* deleted DNA-containing pK18*mobsacB*, Km^r	This study
pK18- Δ*cheA2*	*cheA2* deleted DNA-containing pK18*mobsacB*, Km^r	This study
pK18- Δ*cheY2*	*cheY2* deleted DNA-containing pK18*mobsacB*, Km^r	This study
pDSK519	Broad host range cloning vector, Km^r	Keen *et al*. 1988
pD-*cheA2*	pDSK519 possessing expressible *cheA2*, Km^r	This study
pD-*cheY2*	pDSK519 possessing expressible *cheY2*, Km^r	This study
pD-*cheA1*	pDSK519 possessing expressible *cheA1*, Km^r	This study
pD-*cheY1*	pDSK519 possessing expressible *cheY1*, Km^r	This study

Nal^r, nalidixic acid resistant; Amp^r, ampicillin resistant; Km^r, kanamycin resistant

Table 2 Primer sequences used in this study for DNA cloning and mutant construction

Primer Name	Sequence (5'--3')	Description
*cheA1*_1	ATGGCTAAGAGTGTATTGGTGGTCG	Amplification of *cheA-1* and surrounding region
*cheA1*_2	GTCTCGTCCTTGGAACCGTG	
*cheA1*_3	CGCggatccTGTTGCCCACTTCTCGCTGA	Deletion of *cheA-1* ORF
*cheA1*_4	CGCggatccCTGCTGTGCCTGATCGAGAT	
*cheA2*_1	ACGCTGTGCAGCTGATCCAT	Amplification of *cheA-2* and surrounding region
*cheA2*_2	TGGCAACTGGGTAAGTACCCGT	
*cheA2*_3	CGCggatccCACGGCGTATCTGAACCCGG	Deletion of *cheA-2* ORF
*cheA2*_4	CGCggatccTCATCGGCGCCGAAGCTCAT	
*cheY1*_1	ACCAACCTGCTGGCCCTTAA	Amplification of *cheY-1* and surrounding region
*cheY1*_2	GCGGTCGAGCACGTCTTCAA	
*cheY1*_3	CGCggatccCCAAGCTGATCCTGCCCTGA	Deletion of *cheY-1* ORF
*cheY1*_4	CGCggatccCCACCAATACACTCTTAGCCAT	
*cheY2*_1	GCCGAACTCCAGTTGAGTCT	Amplification of *cheY-2* and surrounding region
*cheY2*_2	CTGGCCATGAGCACCAGTTT	
*cheY2*_3	CGCggatccTCAATAGCTGATGCATGCCG	Deletion of *cheY-2* ORF
*cheY2*_4	CGCggatccTCATGTTCTTGTCCAATTCGACC	
*che2pro*_R	GG*ggtacc*GTTCTTGTCCAATTCGACCTCC	Amplification of *che2* predicted promoter (paired with *cheY2-C*_F) for complementation
*cheA2-C*_F	GG*ggtacc*ATGAGCTTCGGCGCCGAT	Amplification of *cheA2* ORF for complementation
*cheA2-C*_R	ggatccTCAGATACGCCGTGCGGC	
*cheY2-C*_F	ggatccCTGAACCTCAAGGAAATCGG	Amplification of *cheY2* and its predicted promoter region for complementation
*cheY2-C*_R	ggatccCGGCATGCATCAGCTATTGA	
*che1pro*_F	GGCCCGCCAGCCGAGAGG	Amplification of *che1* predicted promoter (paired with *cheA1/Y1pro* for complementation
cheA1pro	TAATACTCACGGGTTCGATCCTTGAACAGT	Amplification of *che1* predicted promoter for seamless attachment to *cheA1* ORF
cheY1pro	TCTTAGCCATGGGTTCGATCCTTGAACAGT	Amplification of *che1* predicted promoter for seamless attachment to *cheY1* ORF
cheA1-C_F	GATCGAACCCGTGAGTATTAATCTCGATCAGGCAC	Amplification of *cheA1* ORF for complementation
cheA1-C_R	TCAGCGAGAAGTGGGCAACA	
cheY1-C_F	GATCGAACCCATGGCTAAGAGTGTATTGGT	Amplification of *cheY1* ORF for complementation
cheY1-C_R	TCAGGGCAGGATCAGCTTGG	

Lowercase letters indicate artificial nucleotide sequence for *Bam*HI in Δ*cheA-1*, Δ*cheA-2*, Δ*cheY-1*, and Δ*cheY-2*, *cheA2-C* and *cheY2-C*. Lowercase italic letters indicate artificial nucleotide sequence for *Kpn*I in *che2* promoter and *cheA2-C*.

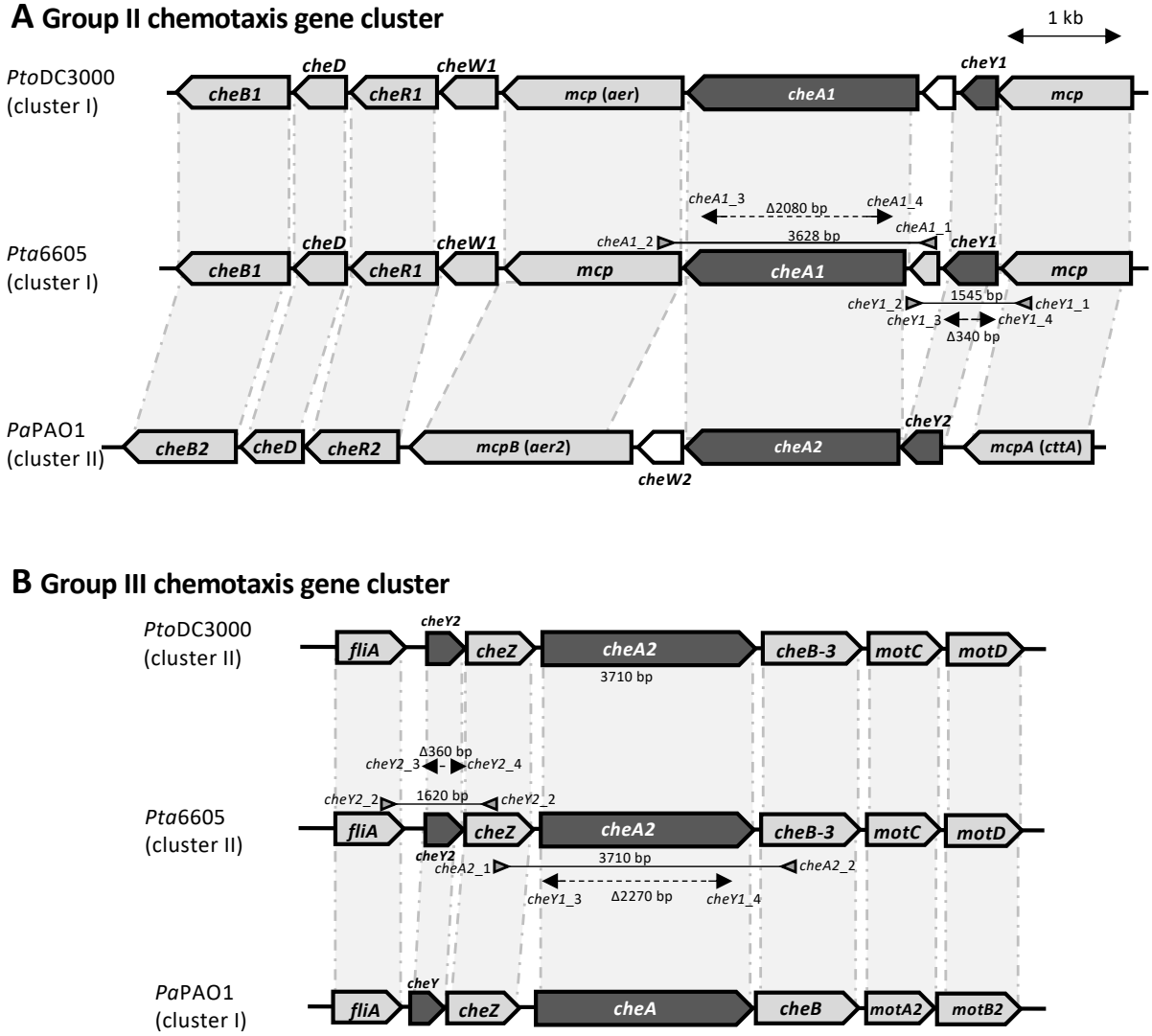

Fig. 1 Chemotaxis gene clusters in *P. syringae* pv. *tomato* (*Pto*) DC3000, pv. *tabaci* (*Pta*) 6605 and *P. aeruginosa* (*Pa*) PAO1. Schematic organization of group II chemotaxis gene clusters including cluster I in *Pto*DC3000 and *Pta*6605, and cluster II in *Pa*PAO1 (**A**), and group III chemotaxis gene clusters including cluster II in *Pto*DC3000 and *Pta*6605, and cluster I in *Pa*PAO1 (**B**). The constructions of the Δ*cheA1*, Δ*cheY1*, Δ*cheA2*, and Δ*cheY2* mutants are also illustrated in *Pta* 6605. Light gray arrowheads indicate the positions of the PCR primers used to clone each *cheA* and *cheY* gene. Each gene name is shown in or above the pentagons. Inverse PCR was carried out to generate ORF-deleted DNA in each gene using primers indicated by dark gray arrowheads.

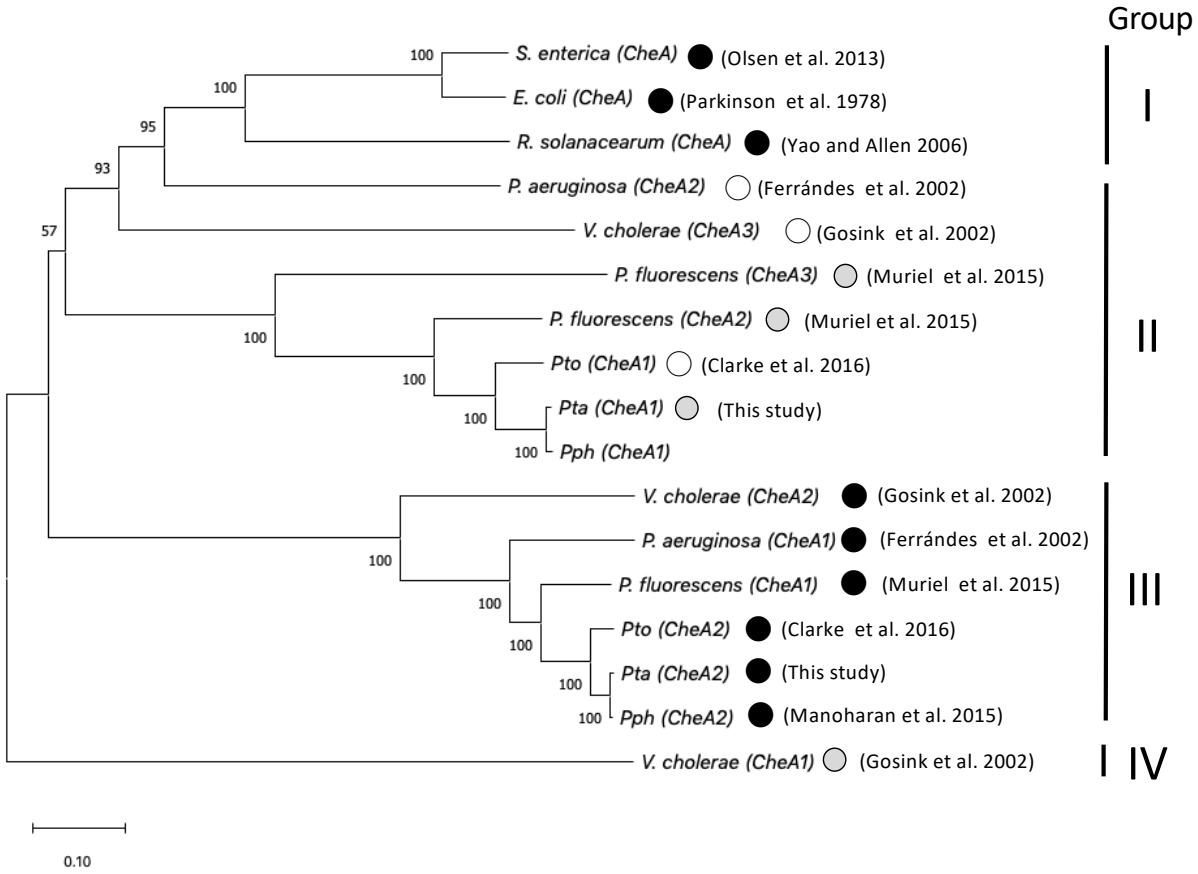

Fig. 2 Phylogenetic tree comparing CheA protein sequences. A neighbor-joining tree based on aligned CheA protein sequences of *Pta*6605, *Pto*DC3000, *Pph*1448A, *R. solanacearum* GMI1000, *P. aeruginosa* PAO1, *E. coli* K-12, *P. fluorescens* F113, *V. cholerae* O395, and *S. enterica* serovar *typhimurium* LT2. Numbers at nodes represent bootstrap support based on 1000 replicates. Evolutionary distances were determined using the Poisson correction method and are in units of the number of amino acid substitutions per site. The tree was generated using MEGA7 software. Circle marks indicate that mutation of *cheA* resulted in lost (black), reduced (gray), or unaffected (white) chemotaxis-related phenotypes. Each reference is also shown on the right.

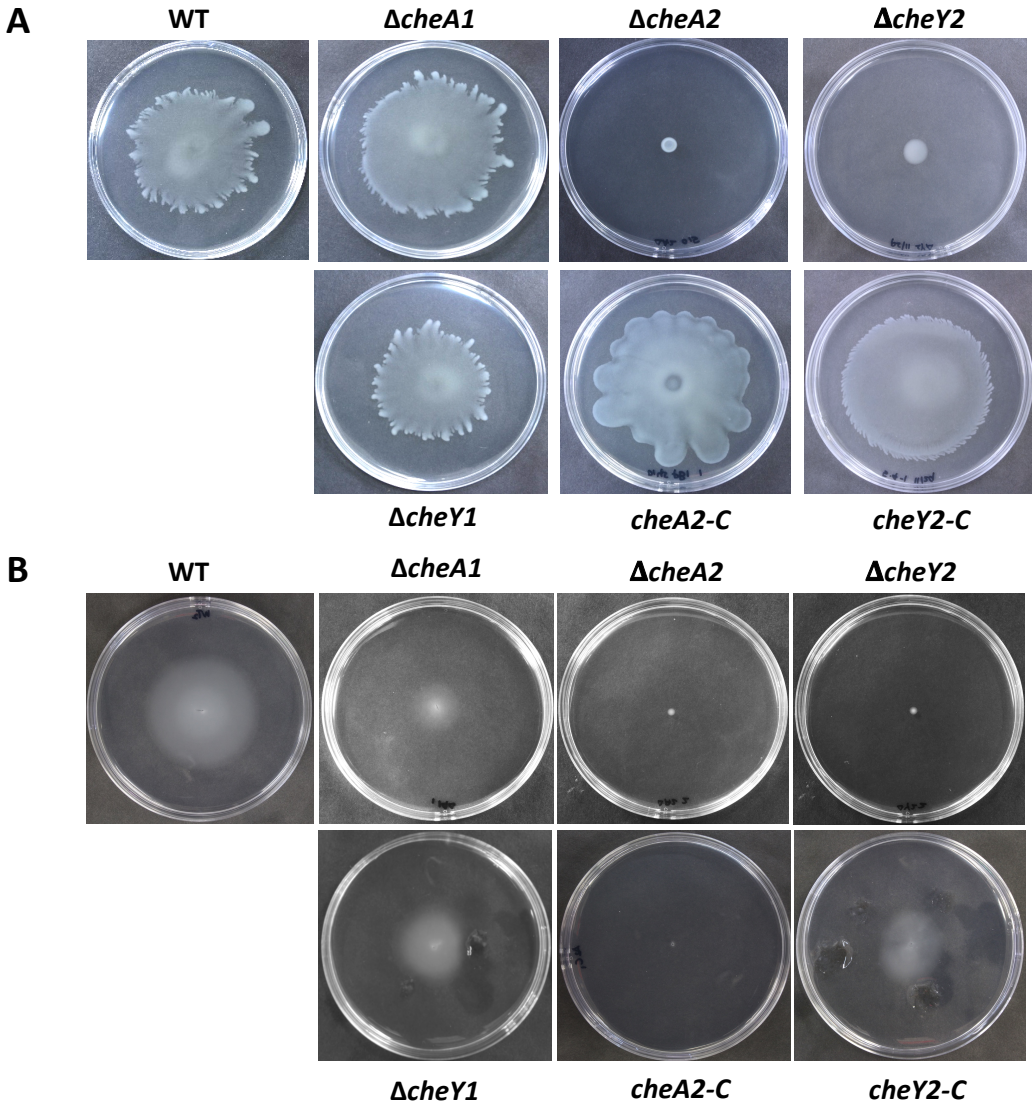

Fig. 3 Surface motility phenotypes of WT and each mutant. (**A**) Surface swarming assay on SWM plates with 0.45% agar at 27°C and (**B**) surface swimming assay on MMMF plates with 0.25% agar at 27°C. Three µl of each bacterial suspension (2×10^8 CFU/ml) was spotted on the center of the plate and incubated for 48 h (swarming) and 72 h (swimming). The photographs show representative results obtained from three independent experiments (each with 2 technical replicates).

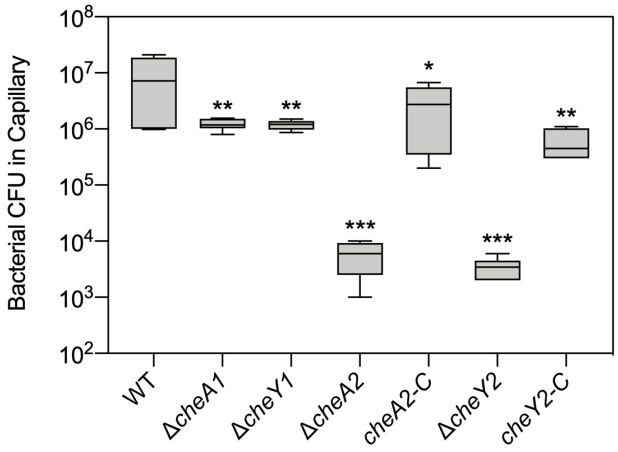

Fig. 4 Quantitative capillary chemotaxis assay of WT and each mutant to 1% yeast extract. The number of bacteria attracted into the capillary was measured in each strain. The experiment was repeated two times with two different colonies of each mutant, and similar results were obtained. Asterisks indicate statistically significant differences between WT and mutant strains (**P* <0.05; ***P* <0.01; ****P* <0.001; by Dunnett's multiple comparisons test). Error bars represent standard errors from two independent experiments (each with three technical replicates).

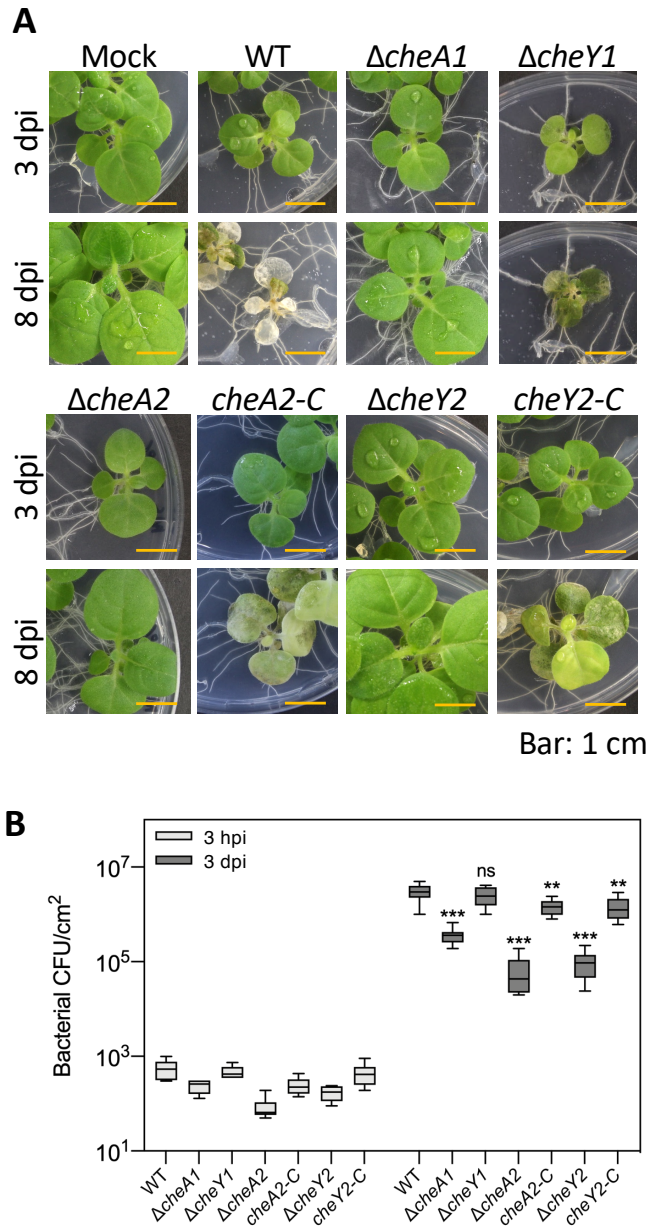

Fig. 5 Inoculation of host tobacco leaves by flood assay method. (**A**) Tobacco seedlings were inoculated by flooding with 8 × 10^6 CFU/ml bacterial suspension of each strain and incubated at 22°C. Photographs taken 3 and 8 dpi show representative results from three independent experiments. (**B**) Bacterial populations were counted at 3 hpi and 3 dpi. The bars represent the standard error from two independent experiments. Bacterial CFUs for each strain in one experiment were pooled from 3 (3 hpi) or 4 (3 dpi) individuals. Asterisks indicate statistically significant differences between WT and mutants (ns: not significant; ***P* <0.01; ****P* <0.001 by Dunnett's multiple comparisons test).

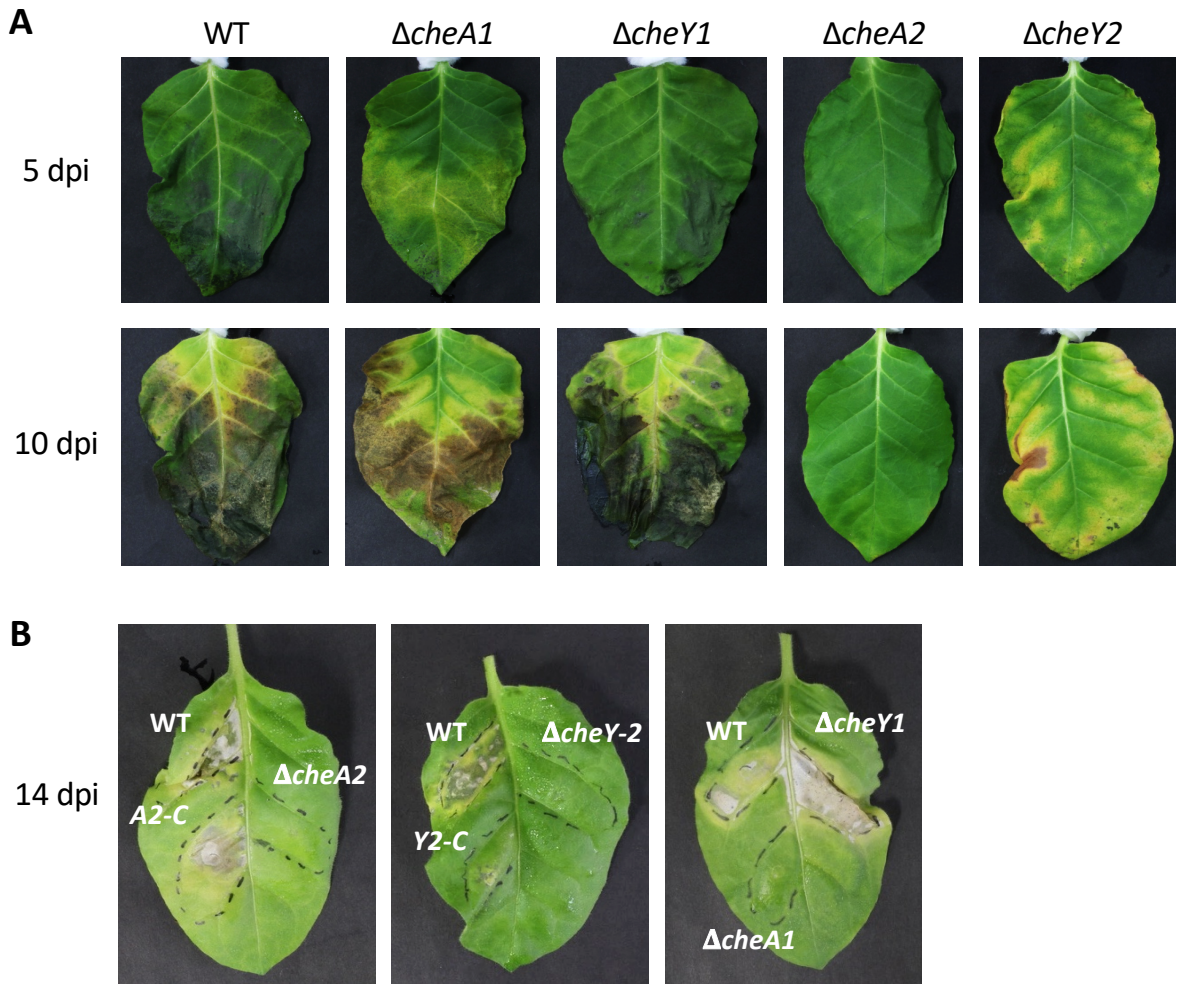

Fig. 6 Dip and infiltration inoculation tests on host tobacco leaves of the WT and each mutant. (**A**) Detached tobacco leaves were inoculated by dipping into 2 × 10^8 CFU/ml bacterial suspension of each strain and incubated at 22°C. Photographs taken 5 and 10 dpi show representative results from three independent experiments. Silwet L-77 was added at 0.04% (v/v) to the bacteria suspension prior to dip-inoculation experiments. Detached leaves of 8-wk-old tobacco plants were dipped into the bacterial suspension for 2 min, placed in a tray, and covered with plastic wrap. Cut petioles were wrapped and supplied water with cotton. (**B**) Attached tobacco leaves of whole plants were infiltrated by 2 × 10^5 CFU/ml of each strain incubated at 22°C. Photographs taken 14 dpi show representative results from two independent experiments. In one experiment, three leaves from independent plants were used for each bacterial strain.

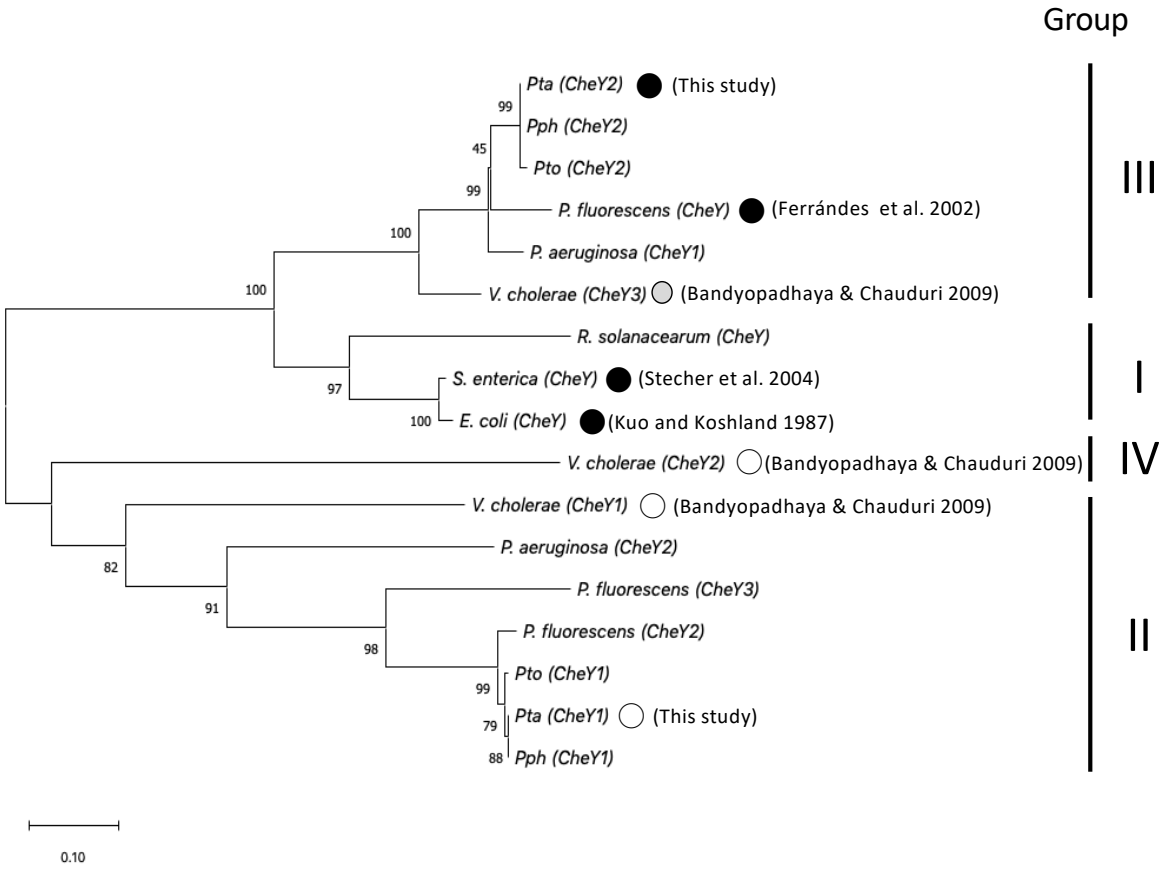

Fig. S1 Phylogenetic tree comparing CheY protein sequences. Neighbor-Joining tree based on aligned CheY protein sequences in *Pta*6605, *Pto*DC3000, *Pspph*1448A, *R. solanacearum* GMI1000, *P. aeruginosa* PAO1, *E. coli* K-12, *P. fluorescens* F113, *V. cholerae* O395, and *S. enterica* serovar *typhimurium* LT2. Number at nodes represent bootstrap support based on 1000 replicates. Evolutionary distances were determined using the Poisson correction method and are in the units of the number of amino acid substitutions per site. The tree was generated using MEGA7 software. A circle mark indicates that mutation of *cheY* resulting in lost (black), reduced (grey), or did not affect (white) chemotaxis related phenotype. Each reference is also shown on the right.

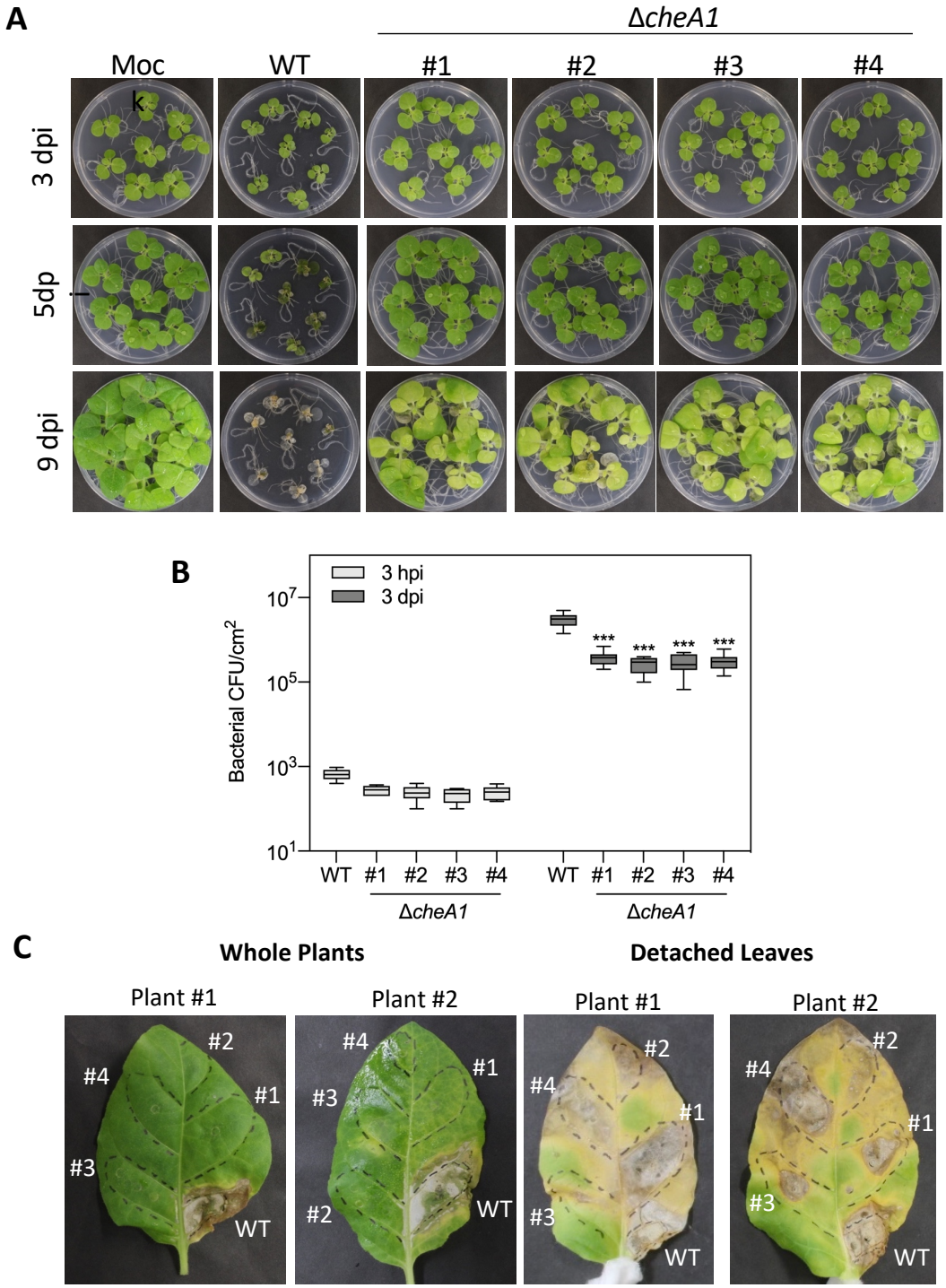

Fig. S2 Flood assay and infiltration inoculation test on host tobacco plants (whole plants and detached leaves) of the WT and Δ*cheA1*. (A) Tobacco seedlings were inoculated by flooding with 8 × 10^6 CFU/ml bacterial suspension of each strain and incubated at 22°C. Photographs taken 3, 5 and 9 dpi show representative results from two independent experiments. **(B)** Bacterial populations were counted at 3 hpi and 3 dpi. The bars represent standard error from two independent experiments. Bacterial CFUs for each strain in one experiment were pooled from 3 (3 hpi) or 4 (3 dpi) individuals. Asterisks indicate statistically significant differences between WT and mutants (***P < 0.001 by Dunnett's multiple comparisons test). **(C)** Tobacco leaves were infiltrated by 2 × 10^5 CFU/ml of each strain and incubated at 22°C. Photographs taken 14 dpi show representative results from two independent experiments. In one experiment, two leaves from two independent plants were used.

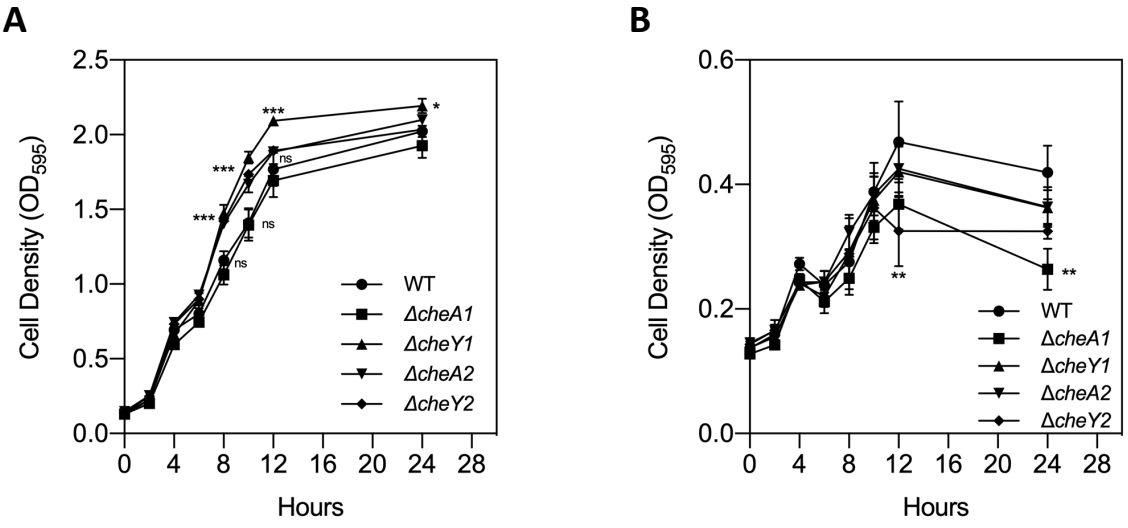

Fig. S3 Growth curves of *P. syringae* pv. *tabaci* 6605 WT and its *che* mutant strains in (A) King's B medium and (B) MMMF medium. Bacterial growth was measured at OD_{595}. Asterisks indicate statistically significant differences between WT and mutants (ns: not significant; **P* < 0.05; ***P* < 0.01; ****P* < 0.001 by Dunnett's multiple comparisons test). Data are means of two independent experiments conducted in triplicate.

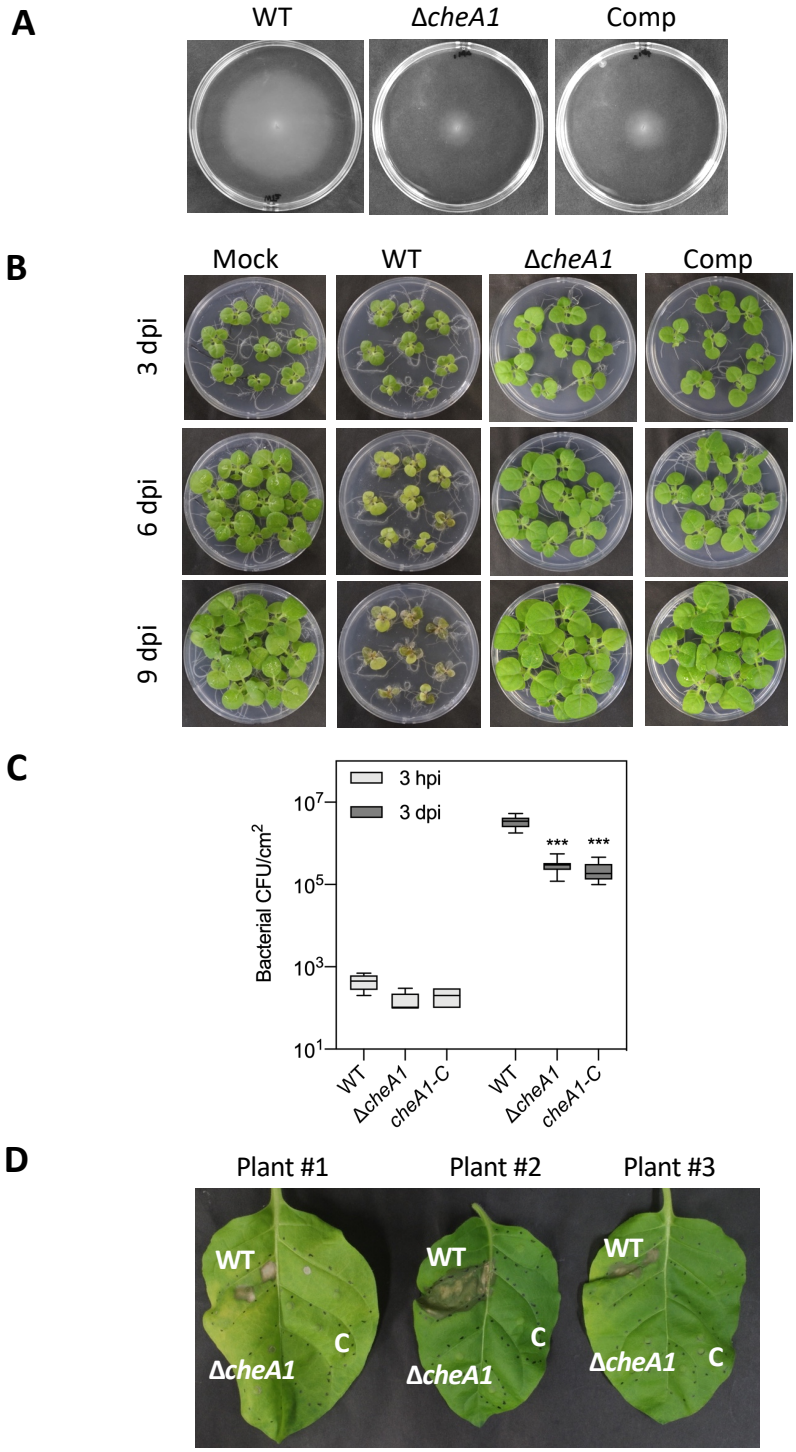

Fig. S4 Swimming motility and virulence of Δ*cheA1* and its complementary strain. (A) Swimming motility on MMMF plates with 0.25% agar at 27°C. Three µl of each bacterial suspension (2 × 10^8 CFU/ml) was spotted on the center of the plate and incubated for 72h. The photographs show representative results obtained from two independent experiments (each with 3 technical replicates). **(B)** Flood assay inoculation. Tobacco seedlings were inoculated by flooding with 8 × 10^6 CFU/ml bacterial suspension of each strain and incubated at 22 ºC. Photographs taken 3, 6 and 9 dpi show representative results from two independent experiments. **(C)** Bacterial populations were counted at 3 hpi and 3 dpi. The bars represent standard error from two independent experiments. Bacterial CFUs for each strain in one experiment were pooled from 3 (3 hpi) or 4 (3 dpi) individuals. Asterisks indicate statistically significant differences between WT and other tested strains (***$P < 0.001$ by Dunnett's multiple comparisons test). **(D)** Tobacco leaves were infiltrated by 2 × 10^5 CFU/ml of each strain and incubated at 22°C. Photographs taken 10 dpi show representative results from two independent experiments. In one experiment, three leaves from three independent plants were used. "C" denotes Δ*cheA1* mutant complemented with *cheA1*.

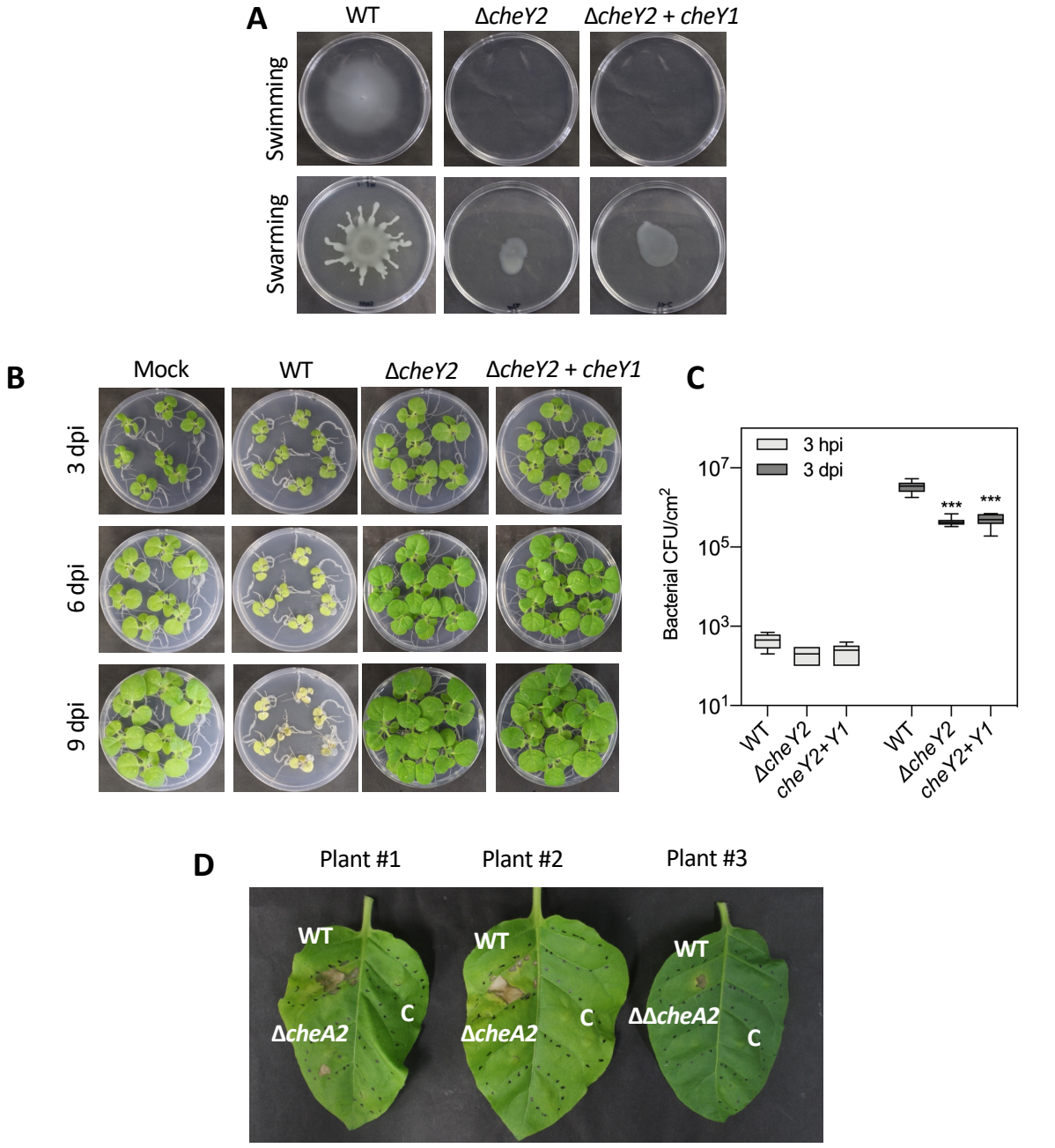

Fig. S5 Effect of *cheY1* overexpression in *cheY2* mutant. (A) Swimming (MMMF plates with 0.25% agar) and swarming motilities (SWM plates with 0.45% agar) at 27°C. Three µl of each bacterial suspension (2 × 10^8 CFU/ml) was spotted on the center of the plate and incubated for 72h (swim) and 48h (swarm). The photographs show representative results obtained from two independent experiments (each with 3 technical replicates). **(B)** Flood assay inoculation. Tobacco seedlings were inoculated by flooding with 8 × 10^6 CFU/ml bacterial suspension of each strain and incubated at 22°C. Photographs taken 3, 6 and 9 dpi show representative results from two independent experiments. **(C)** Bacterial populations were counted at 3 hpi and 3 dpi. The bars represent standard error from two independent experiments. Bacterial CFUs for each strain in one experiment were pooled from 3 (3 hpi) or 4 (3 dpi) individuals. Asterisks indicate statistically significant differences between WT and other tested strains (***$P < 0.001$ by Dunnett's multiple comparisons test). **(D)** Tobacco leaves were infiltrated by 2 × 10^5 CFU/ml of each strain and incubated at 22°C. Photographs taken 10 dpi show representative results from two independent experiments. In one experiment, three leaves from three independent plants were used. "C" denotes Δ*cheY2* mutant complemented with *cheY1*.

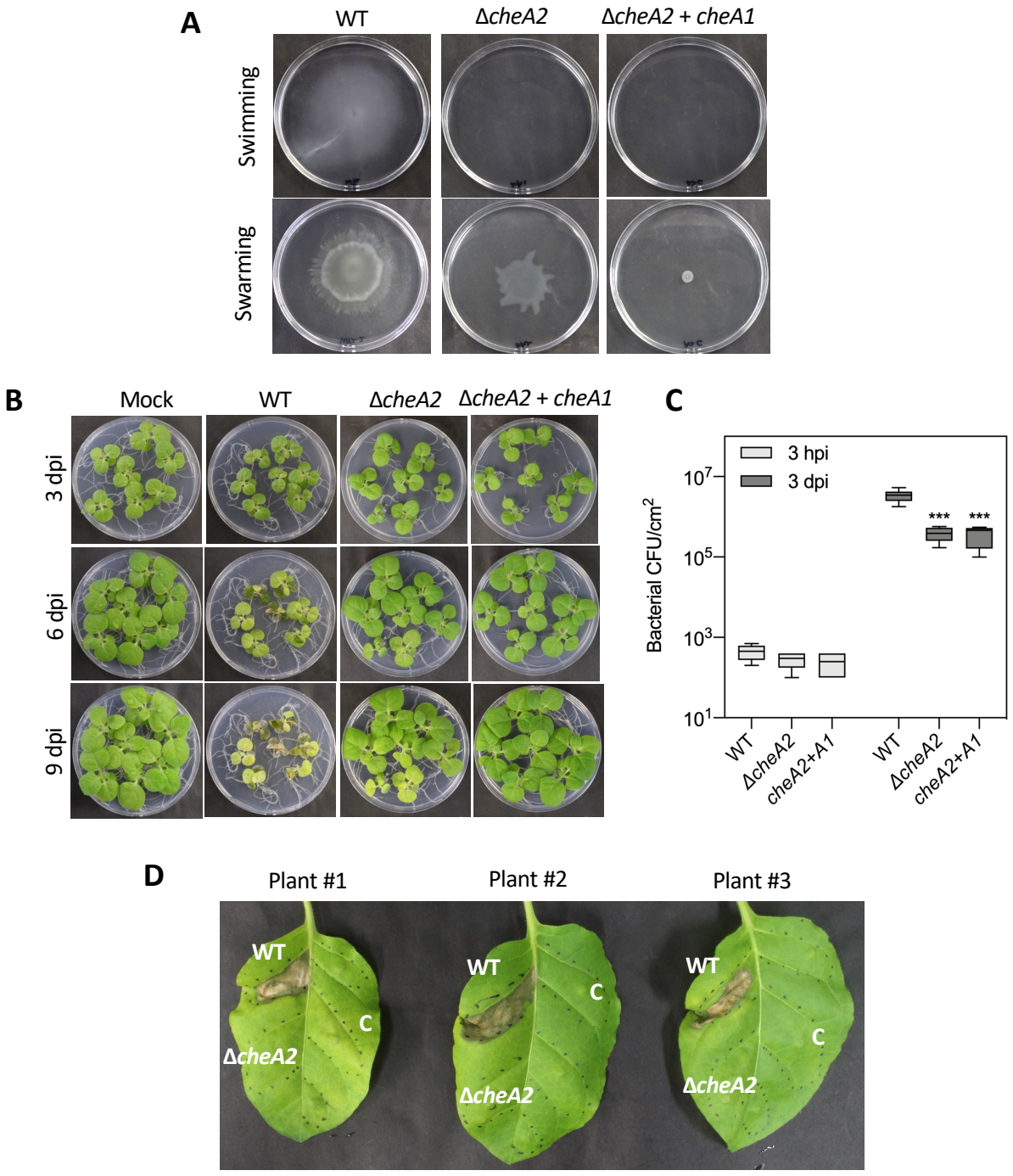

Fig. S6 Effect of *cheA1* overexpression in *cheA2* mutant. (A) Swimming (MMMF plates with 0.25% agar) and swarming motilities (SWM plates with 0.45% agar) at 27°C. Three µl of each bacterial suspension (2 × 10^8 CFU/ml) was spotted on the center of the plate and incubated for 72h (swim) and 48h (swarm). The photographs show representative results obtained from two independent experiments (each with 3 technical replicates). **(B)** Flood assay inoculation. Tobacco seedlings were inoculated by flooding with 8 × 10^6 CFU/ml bacterial suspension of each strain and incubated at 22°C. Photographs taken 3, 6 and 9 dpi show representative results from two independent experiments. **(C)** Bacterial populations were counted at 3 hpi and 3 dpi. The bars represent standard error from two independent experiments. Bacterial CFUs for each strain in one experiment were pooled from 3 (3 hpi) or 4 (3 dpi) individuals. Asterisks indicate statistically significant differences between WT and other tested strains (***$P < 0.001$ by Dunnett's multiple comparisons test). **(D)** Tobacco leaves were infiltrated by 2 × 10^5 CFU/ml of each strain and incubated at 22°C. Photographs taken 10 dpi show representative results from two independent experiments. In one experiment, three leaves from three independent plants were used. "C" denotes Δ*cheA2* mutant complemented with *cheA1*.